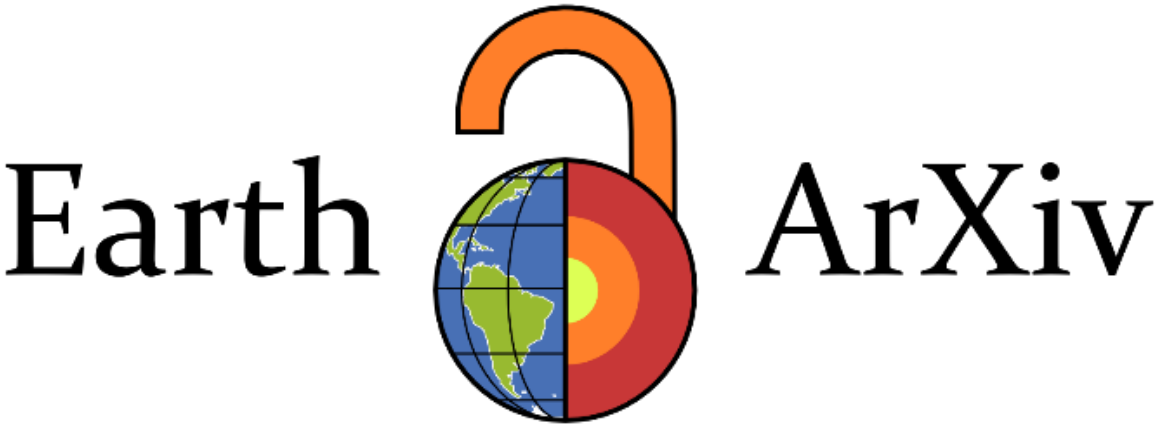

Evaluating Urban Heat Adaptation Strategies for Extreme Heatwaves in Complex Terrain: A Case Study of Grenoble, France

Jacobo Gabeiras[1], Chantal Staquet[1], Charles Chemel[2], Alberto Martilli[3]

[1]Université Grenoble Alpes, CNRS, Grenoble INP, LEGI, France
[2]National Centre for Atmospheric Science, NCAS, Leeds, UK
[3]Centro de Investigaciones Energéticas, Medioambientales y Tecnológicas, CIEMAT, Spain

Abstract. Urban heat adaptation strategies are critical for mitigating the impacts of extreme heat events in cities, particularly as climate change exacerbates their intensity and frequency. This study evaluates a set of adaptation strategies during the 2023 heatwave in Grenoble, France, using the WRF model with the BEP+BEM urban canopy scheme. Eight scenarios are simulated, including increased vegetation, reflective surfaces, enhanced building insulation, permeable surfaces, and combined strategies, assessing their effects on air temperature, thermal comfort (UTCI), and energy demand. The results highlight that strategies involving vegetation, reflective surfaces, and building insulation are particularly effective in reducing temperatures and improving thermal comfort, with tree-based interventions showing the greatest impact. Combined strategies enhance these effects, providing near-additive reductions in heat stress, especially during the day, and improving both outdoor and indoor conditions. Building-focused interventions (e.g. insulation) significantly lower energy demand, whereas ground-based strategies (e.g. permeable ground) primarily improve outdoor thermal comfort. Urban morphology strongly influences the effectiveness of these measures, with densely built areas benefiting the most. This work emphasizes the importance of integrating diverse strategies to address urban heat, bridging immediate mitigation efforts with long-term resilience planning.

1 Introduction

The frequency, intensity, and duration of heatwaves are increasing worldwide due to climate change, posing serious threats to urban populations (Perkins et al., 2012; Perkins-Kirkpatrick & Lewis, 2020). Urban areas now house over 56% of the global population and, according to the United Nations (UN), this percentage is projected to grow up to 68% by 2050 (United Nations Department of Economic and Social Affairs, 2019). These areas are particularly vulnerable to extreme heat events, with this risk projected to grow alongside continued urbanization (Liao et al., 2018; Marcotullio et al., 2022). Cities experience exacerbated heating compared to rural regions primarily due to the Urban Heat Island (UHI) effect, a phenomenon where urban surfaces absorb and retain more heat, typically caused by limited vegetation, dense infrastructure, and anthropogenic heat emissions contributing to sustained high temperatures (Hatvani-Kovacs & Boland, 2015; Renard et al., 2019).

Studies have shown that extreme heat events significantly affect public health, energy infrastructure, and urban livability, often with severe implications for densely populated areas. The 2003 European heatwave, resulted in approximately 70,000 excess deaths across Europe, with significant mortality reported in cities like Paris (X. Y. Wang et al., 2012). While such an event was considered rare at the time, similar heatwaves have become increasingly frequent. In 2022, Europe experienced a series of heatwaves, leading to over 61,600 heat-related deaths (Ballester et al., 2023). The summer of 2023 continued this trend, with widespread extreme heat across

the continent, showcasing the escalating frequency and intensity of such events (Gallo et al., 2024).

To address these growing challenges, researchers have explored various adaptation strategies to mitigate urban heat and enhance resilience, such as increasing vegetation, optimizing urban ventilation, and improving building insulation (Han et al., 2023; Larsen, 2015). However, the effectiveness of these strategies can vary widely depending on local climate, urban morphology, and infrastructure (H. Li et al., 2024; V. Schmidt, 2024). It is thus important to assess adaptation strategies within specific urban contexts, especially for cities with unique geographic and climatic conditions such as Grenoble.

Weather models, particularly the Weather Research and Forecasting (WRF) model, have been applied extensively to study urban heat distribution and evaluate adaptation measures. When coupled with the urban model BEP+BEM (Building Effect Parameterization (Martilli et al., 2002) and Building Energy Model (Salamanca et al., 2010)), WRF can simulate complex interactions between urban forms, materials, and vegetation, offering detailed insights into how adaptation scenarios impact temperature, energy use, and comfort (Martilli et al., 2024; Pappaccogli et al., 2021). The use of thermal comfort indices, such as the Universal Thermal Climate Index (UTCI), have become increasingly popular for quantifying adaptation effectiveness, as they provide a comprehensive measure of outdoor comfort (Bröde et al., 2012; Mazdiyasni et al., 2019).

In this study, high resolution simulations are made (200 meter of grid cell size), focusing on Grenoble, a city with distinctive geographic and urban characteristics that heighten its vulnerability to heat. Using WRF, the latest version of BEP+BEM urban canopy model, and the COMFORT module for UTCI calculation, this research evaluates different adaptation strategies through several individual and combined adaptation scenarios during the 2023 heatwave in Grenoble. To accurately represent the urban environment, we applied the World Urban Database and Access Portal Tools (WUDAPT) Local Climate Zone (LCZ) generator, and integrated detailed urban parameters by use of the WRFUP tool (Gabeiras, 2024), which sources advanced settlement data from the World Settlement Footprint 3D (WSF3D) dataset (Esch et al., 2022), Global Urban Fraction (Patel & Roth, 2022) and the Global UrbanSurfAce dataset (Gabeiras, 2025). This analysis, conducted in collaboration with The Grenoble Alpes Métropole and the Agency of Urbanism of Grenoble (AURG), aligns with local adaptation policies. While serving as a proof of concept, it aims to inform about strategies for future climate resilience in urban areas facing similar challenges. Specifically, this study investigates: (1) the effectiveness of different urban heat adaptation strategies in reducing air temperature and improving outdoor thermal comfort during a extreme heat event, (2) the relative performance of these strategies in mitigating nighttime heat retention and energy demand in a dense urban environment, and (3) the combined effects of multiple adaptation strategies and their interactions.

The remainder of this paper is structured as follows. Section 2 reviews key adaptation strategies for mitigating extreme urban heat. Section 3 describes the methodology, including the study area, heatwave characterization, model configuration, urban parameter integration, model validation, and the design of adaptation scenarios. Section 4 presents the control run results, providing a baseline for comparison. Section 5 discusses the results of individual adaptation scenarios, focusing on their effects on temperature, UTCI, and energy consumption. Section 6 presents the results of combined adaptation scenarios, evaluating their effectiveness in reducing temperature, improving thermal comfort, and decreasing energy demand. Section 8 interprets these findings, discussing broader implications for urban adaptation policies and model limitations. Finally, Section 9 summarizes key conclusions and suggests directions for future research. Additional details, data, and supplementary analyses are provided in the appendix (Section 10).

2 Adaptation Strategies Review

Adaptation strategies to extreme heat in mid-latitude cities can be effectively categorized into three groups: green strategies, gray strategies, and soft strategies (ADEME, 2020). Each category includes various approaches that aim to mitigate the impacts of extreme heat on urban populations, particularly concerning health, UHI effects, and energy consumption.

Green Adaptation Strategies

Green strategies focus on enhancing urban greenery and water features to combat heat. Urban greening, which includes planting trees and increasing green spaces, has been shown to effectively reduce surface temperatures through shade provision and evapotranspiration, thereby lowering the UHI effect (Knight et al., 2021). For instance, studies indicate that urban vegetation can significantly improve thermal comfort for pedestrians by reducing mean radiant temperatures (Knight et al., 2021). Green roofs and walls contribute to this cooling effect by insulating buildings and reducing heat absorption, which can lead to decreased energy consumption for cooling (Alexandri & Jones, 2008). Permeable surfaces facilitate water infiltration and evaporation, further promoting cooling in urban areas (Haroun et al., 2022). Additionally, the incorporation of water features, such as fountains and ponds, can enhance airflow and provide localized cooling, thus improving overall urban climate resilience (Yuan, 2024).

Green strategies synergistically improve public health by reducing heat-related illnesses, particularly among vulnerable populations like the elderly and children (Balany et al., 2020). The integration of green infrastructure not only addresses thermal comfort but can also enhance biodiversity, improve air quality and overall physical and mental health, creating a multifaceted approach to urban resilience (Balany et al., 2020; Blessing Aibhamen Edeigba et al., 2024; K. Schmidt & Walz, 2021).

Gray Adaptation Strategies

Gray strategies involve the use of engineered solutions to mitigate heat impacts. Cool roofs and pavements, which utilize high-albedo materials, reflect sunlight and reduce heat absorption, thus effectively lowering surface temperatures (Lee et al., 2023; D. Li et al., 2014). Research has shown that cool roofs and pavements can reduce surface temperatures by up to 15.5°C and 11.6°C, respectively, while also lowering air temperatures by 1°C to 2°C (Y. Wang et al., 2016). Building insulation improvements are also crucial for maintaining cooler indoor environments and reducing energy demand during heatwaves (D. Li et al., 2014). The installation of solar panels not only generates renewable energy but also provides shading, thereby reducing heat loads on buildings (Dominguez et al., 2011). Shading structures, such as awnings and canopies, further enhance outdoor comfort by minimizing direct solar exposure (Kwon & Lee, 2017). The effectiveness of gray strategies is amplified when combined with green strategies, as the latter can help to lower ambient temperatures further, enhancing the overall cooling effect (Van Oorschot et al., 2024). Moreover, these strategies can significantly reduce energy consumption, specially those with direct action on buildings, potentially leading to lower greenhouse gas emissions and improved urban air quality (D. Li et al., 2014).

Soft Adaptation Strategies

Soft strategies include policy and community-based approaches aimed at enhancing resilience to extreme heat. Community awareness programs play an important role in educating residents about the health impacts of extreme heat and promoting energy conservation practices (Hasan et al., 2021). Early warning systems for informing the public about impending heat events,

allow for timely protective actions (Lowe et al., 2011). Incentive programs can encourage the adoption of green and gray strategies by providing financial support for energy-efficient upgrades and green infrastructure (Razzak et al., 2022).

In conclusion, the holistic integration of green, gray, and soft adaptation strategies is needed to address extreme heat in mid-latitude cities. Each strategy contributes uniquely to reducing health risks, lowering temperatures, mitigating the UHI effect, and decreasing energy consumption. The synergistic effects of these strategies can enhance urban resilience, ultimately leading to healthier and more sustainable urban environments.

3 Methodology

3.1 Area of Study

Grenoble, located in southeastern France, is highly vulnerable to extreme heat due to its unique geographical and urban characteristics. The city is situated in a narrow alpine valley surrounded by mountain ranges, as a result, ventilation is controlled by topography and is therefore more limited than on an open surface. Also, during heatwaves, solar heating affects not only the valley floor but also the surrounding mountain slopes, thereby strongly increasing the total heated surface area of the valley volume compared to the same volume over a plain. This topographical feature amplifies the urban heat island (UHI) phenomenon, particularly during heatwaves, leading to prolonged periods of elevated temperatures in the city center compared to surrounding rural areas (Zhu et al., 2024).

Home to approximately 450,000 inhabitants, Grenoble is one of the most polluted cities in France, with air quality challenges exacerbated by its geographical setting, traffic, and reliance on combustion-based heating systems (Métropole, 2023). The city's rapid urbanization throughout the 20th century led to the construction of a significant number of buildings with poor insulation, further intensifying heat retention. According to the Grenoble Energy-Climate Roadmap 2050, 42% of the city's total energy consumption is attributed to buildings, many of which were built between 1945 and 1970, requiring substantial energy for cooling and heating (Métropole, 2018). This widespread use of inefficient materials contributes to higher indoor and outdoor temperatures during heatwaves, increasing energy demand and straining local energy infrastructure.

Furthermore, Grenoble's dense urban morphology, characterized by a high concentration of impervious surfaces such as asphalt and concrete, intensifies the UHI effect. The limited presence of green spaces and vegetation reduces the cooling benefits of evapotranspiration and shade, making urban heat mitigation more challenging. In response, the city has prioritized adaptation strategies such as urban greening, building retrofitting, and the expansion of its district heating system to transition towards more sustainable energy solutions (Métropole, 2018).

Grenoble has been a pioneer in climate action, being the first French metropolis to elect a Green mayor and establishing ambitious energy and climate policies. It has been a signatory of the Covenant of Mayors since 2008 and has committed to reducing greenhouse gas emissions by 75% and achieving 100% renewable energy by 2050 (Métropole, 2018). To address the growing UHI issue, the metropolitan government deployed in 2020 a network of 160 temperature sensors across 27 municipalities to monitor and mitigate urban overheating (Métropole, 2023). Additionally, the city is implementing measures such as increasing tree cover, promoting building insulation, and reducing fossil fuel dependency to enhance climate resilience.

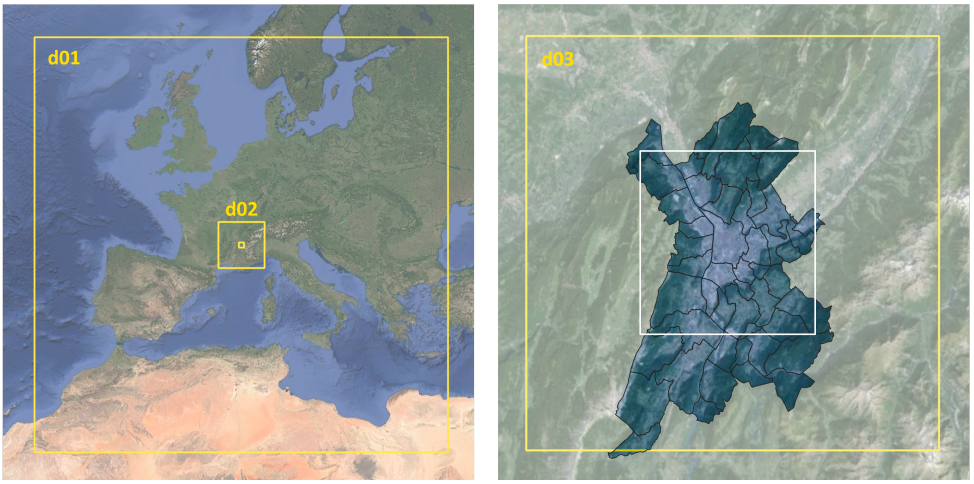

Figure 1: Study area and simulation domains for the 2023 Grenoble heatwave analysis. The left panel shows the nested domains used in the Weather Research and Forecasting (WRF) model: d01 (9 km resolution) covers Europe and the Mediterranean, d02 (1 km resolution) focuses on southeastern France, and d03 (200 m resolution) centers on Grenoble. The right panel highlights Grenoble Métropole, which includes 49 municipalities and about 450,000 inhabitants. The white square marks the area of the figures in this study, covering over 93% of the population.

3.2 Heatwave Characterization of Event in August 2023

The heatwave that swept across Europe in August 2023 was driven by a persistent high-pressure system that settled over much of Western Europe, resulting in a prolonged period of extreme heat. According to the Copernicus Climate Change Service, August 2023 was the warmest August on record globally, with several regions in southern Europe experiencing temperatures exceeding historical averages, and some areas recording their highest temperatures on record (Copernicus Climate Change Service, 2023).

In France, the heatwave in August 2023 was particularly severe. On August 22, the nationwide average temperature over 24 hours reached 27.1°C, marking the highest late-summer average since records began in 1947 (ClimaMeter, 2023). The extreme heat had profound implications for public health, contributing to an estimated 5,167 excess deaths across the country, particularly among vulnerable populations such as the elderly and those with pre-existing health conditions (Le Monde, 2024). The demand for cooling solutions surged, placing significant strain on energy infrastructure. While specific data on energy consumption during this period is limited, it is well-documented that heatwaves increase electricity demand due to widespread use of air conditioning and cooling systems, leading to challenges in energy supply and distribution, especially during prolonged periods of extreme heat (Le Monde, 2023). In Grenoble, the heatwave had notable local impacts. Daily maximum temperatures exceeded 35°C for 15 consecutive days between the 11th and the 25th, with temperatures surpassing 40°C between the 20th and 24th. Daily minimum temperatures stayed above 18.5°C the whole episode and 20°C between the 21st and 25th (Réseau d'Observation Météorologique du Massif Alpin (ROMMA), 2023).

To identify the 2023 heatwave period, historical temperature records from the Grenoble airport meteorological station were analyzed. Heatwave days were defined using three methodologies for comprehensive comparison. First, according to Meteo France's criteria (Schneider, 2022), the heatwave spanned 14 days, from August 11th to August 25th (Météo-France, 2023). The second method, using the excess heat factor (EHF) approach (Nairn & Fawcett, 2014), identifying heatwave days with mean daily temperatures above the 90th percentile, calculated using a 15-day centered moving window, the event occurred from August 18th to August 24th.

The third method classified heatwave days as those with both maximum and minimum temperatures exceeding the 98th percentile which occurred between August 20th to August 24th. While different methodologies define the heatwave period slightly differently, the period starting in August 18th to the 24th was chosen as indicated by the EHF method. The simulations were run from 17th to the 23rd to simulate uniquely clear sky days allowing for one day spin-up for the WRF model.

3.3 Model Configuration

WRF's high spatial resolution and adaptability make it an effective tool for simulating urban heat dynamics in complex terrains. The model configuration consists of three nested domains with one-way nesting 1. The outermost domain, with a 9 km grid cell resolution, captures regional weather patterns across a large area. Within this, an intermediate domain at 1 km resolution focuses on the Grenoble metropolitan area. The innermost domain, which centers on the Grenoble urban region, has a 200 m resolution to capture fine-scale topography, geographic diversity, urban features, and their consequence on the UHI effect. The vertical dimension is set with 61 pressure levels, and a first mass point height at 2.3 meters.

To accurately represent urban characteristics, the WRF model integrates the BEP+BEM urban canopy model (Salamanca et al., 2010), a multi-layer scheme that includes anthropogenic heat sources, urban structures, and energy exchanges. In its latest version (Martilli et al., 2024), the COMFORT module is incorporated to calculate the UTCI. To simulate vertical mixing and turbulence in dense urban areas, we employed the Bougeault and Lacarrère (BouLac) planetary boundary layer (PBL) scheme (Bougeault & Lacarrere, 1989). In the three domains short-wave and long-wave radiation area parameterized using the Rapid Radiative Transfer Model (Mlawer et al., 1997).

3.4 Urban Parameter Integration

High-resolution urban morphology data was integrated to improve the accuracy of the Weather Research and Forecasting (WRF) model in representing Grenoble's urban and natural landscapes.

The Land Use Index field (LU_INDEX) was derived by combining urban and natural surface datasets. For urban areas, Local Climate Zones (LCZ) were generated using the LCZ generator provided by the World Urban Database and Access Portal Tools (WUDAPT) project (Demuzere et al., 2019, 2021). This tool enabled a customized classification of Grenoble's urban features, incorporating key thermal, geometric, and radiative properties 2. For natural surfaces, the Corine Land Cover (CLC) dataset was utilized and remapped into the United States Geological Survey (USGS) classification system to ensure compatibility with the WRF model. This integration allowed for a seamless representation of both urban and natural landscapes in the LU_INDEX field. Table AT2 illustrates the mapping process between CLC and USGS classifications.

The urban parameters were incorporated in the model using the WRFUP Python package (Gabeiras, 2024), which sources data from advanced datasets like the World Settlement Footprint 3D (WSF3D) (Esch et al., 2022), and the Global Urban Fraction dataset (Patel & Roth, 2022). These parameters are ingested into the WRF `geo_em` files within the WRF Preprocessing System, enabling a detailed representation of urban morphology, including building heights, building planar area, and wall surface. The accurate representation of these urban parameters is important when simulating scenarios where the implementation depends on them. Examples of this are green roofs, cool roofs or plantation of trees, where the application directly depends on parameters such as the total roof or street area.

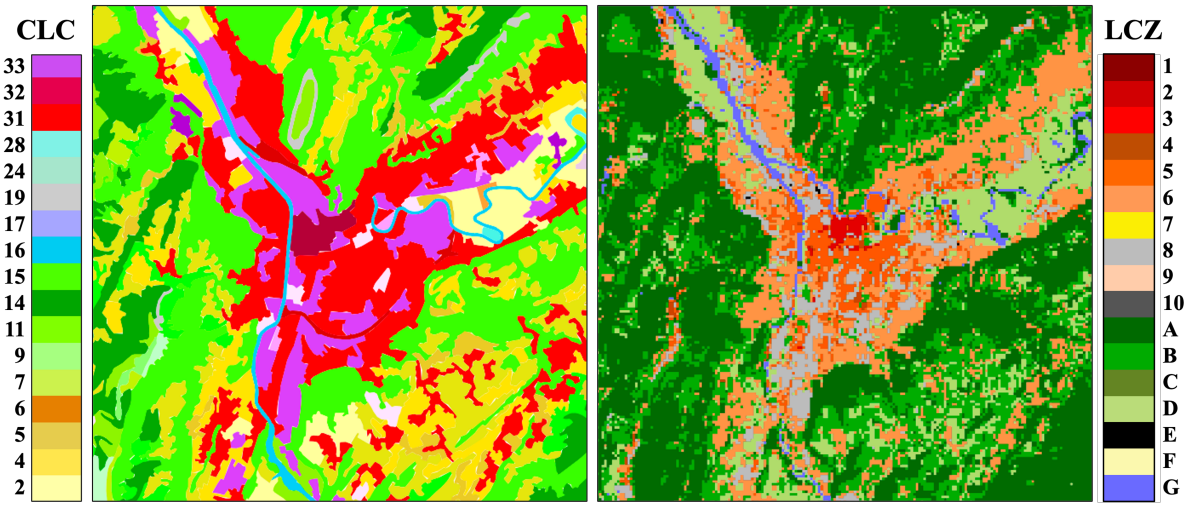

Figure 2: Comparison of the Land cover output using the Corine Land Cover EU database (European Environment Agency, 2019) (left) and the LCZ generator product (Demuzere et al., 2021) (right). The color legend for the CLC map corresponds to the remapped values of the USGS land description (See Table AT2).

3.5 Design and Implementation of Adaptation Scenarios

This study evaluates eight adaptation scenarios to mitigate urban heat, enhance thermal comfort, and reduce energy demand during extreme heat events. The scenarios were designed with the input from local authorities and urban planners in the Grenoble Metropole, ensuring their relevance to local challenges, urban morphology, and policy priorities. While the scenarios unavoidably differ in feasibility and implementation costs, efforts were made to select options with reasonably comparable levels of practical complexity to allow for a balanced assessment of their effectiveness.

The scenarios, along with their parameterization within the WRF model, are as follows:

- **40% Tree Coverage (Trees40):** This scenario increases tree cover in streets to 40% of the available street space not occupied by buildings or existing vegetation. The additional tree cover is parameterized using the latest version of the BEP+BEM+COMFORT urban model, which incorporates shading effects to reduce surface heat storage.
- **30% Permeable Ground (PermGround30):** Aimed at enhancing water infiltration and evaporation, an additional 30% of street surfaces are set as permeable grass. The calculation for available space mirrors that of the Trees40 scenario, and this modification is simulated as grass cover within the urban model, analogous to the green roof parameterization but applied at ground level.
- **Water-Saturated Ground (WetGround):** This scenario increases evaporative cooling by saturating the ground to its water-holding capacity. Unlike the other urban-focused scenarios, this intervention is implemented through adjustments of the initial soil moisture content, setting it to saturation levels based on soil type using WRF soil parameter table (SOILPARM.TBL).
- **Cool Roofs (ALB06):** High-albedo roofs are implemented across all buildings in urban areas, increasing reflectivity from real values of around 0.15 to 0.6. This is parameterized

in the BEP module of the WRF model to reduce rooftop heat absorption and improve building energy efficiency.

- **Insulated Buildings (IsoBuild70):** Building insulation is enhanced by reducing the thermal conductivity of roofs and walls by 70% and decreasing their heat capacity by 5%. These changes are based on typical values for well-insulated materials in industry. The adjustments are parameterized in the urban BEP module to simulate reduced indoor-outdoor heat transfer, thereby lowering energy demand during the heatwave.
- **37% Air Conditioning Usage (AC37):** This scenario reflects the current level of air conditioning usage in Grenoble, where 37% of households are equipped with air conditioning, as opposed to 100% in the rest of the simulations. This adjustment allows for a comparison of energy demand and urban heat impacts between current and full air conditioning penetration. It is implemented using the BEM module of the WRF model.
- **Solar Panels (SP50):** Solar panels are installed on 50% of total roof surfaces, reducing rooftop heat absorption and generating renewable energy. This scenario is parameterized using the BEM module, capturing the cooling benefits and energy production during the heatwave.
- **Green Roofs (GR50):** Sedum cover is applied to 50% of rooftops, improving evaporative cooling and providing insulation benefits. This parameterization is implemented using the BEM module with vegetation types typical for urban green roofs in the region.

These scenarios represent a diverse yet complementary range of adaptation strategies, addressing urban heat mitigation through mechanisms such as shading, increased reflectivity, enhanced insulation, and changes in energy use. Each scenario was simulated independently and compared to the control run to assess its effects on surface temperatures, the urban heat island (UHI) effect, the Universal Thermal Climate Index (UTCI), and cooling-related energy demand.

The analysis is performed separately for daytime and nighttime conditions. This distinction is made as the mechanisms driving urban heat dynamics vary significantly between these periods. During the day, solar radiation dominates, influencing surface heating and thermal comfort. At night, retained heat in urban materials exacerbates the UHI effect, affecting minimum temperatures and cooling energy demand. By evaluating both periods, this study provides a comprehensive understanding of how each adaptation strategy performs under different thermal conditions.

4 Control Run Results and Validation

The control run provides a baseline of near-surface temperature (T_2) during the heatwave episode, capturing both spatial and temporal variations across the study area. Figure 3 illustrates key characteristics of the temperature distribution, highlighting the impacts of urbanization and topography on the thermal environment.

The spatial maps of average maximum and minimum temperatures (Figure 3, top row) show higher maximum temperatures and reduced nighttime cooling in low altitude urban areas compared to rural and elevated regions. Urban areas retain more heat during the night due to their thermal properties, while rural and mountainous regions benefit from more effective cooling. This highlights the role of topography and land use in shaping thermal dynamics during extreme events.

The bottom panel presents box-and-whisker plots of daily minimum and maximum 2-meter temperature for each day of the episode, separated by Local Climate Zone (LCZ). Only five LCZs

(2, 4, 5, 6, 8) are present in the domain. On average, LCZ 2 exhibits the highest minimum and maximum temperatures (24.5°C and 35.4°C, respectively), followed closely by LCZ 8 (23.3°C and 35.3°C). Meanwhile, LCZ 4 has the lowest average minimum (22.5°C), and LCZ 6 shows a relatively lower average maximum (33.8°C). The table alongside the plot summarizes these overall average minimum and maximum temperatures for each LCZ, illustrating how certain LCZs consistently experience higher or lower values throughout the episode.

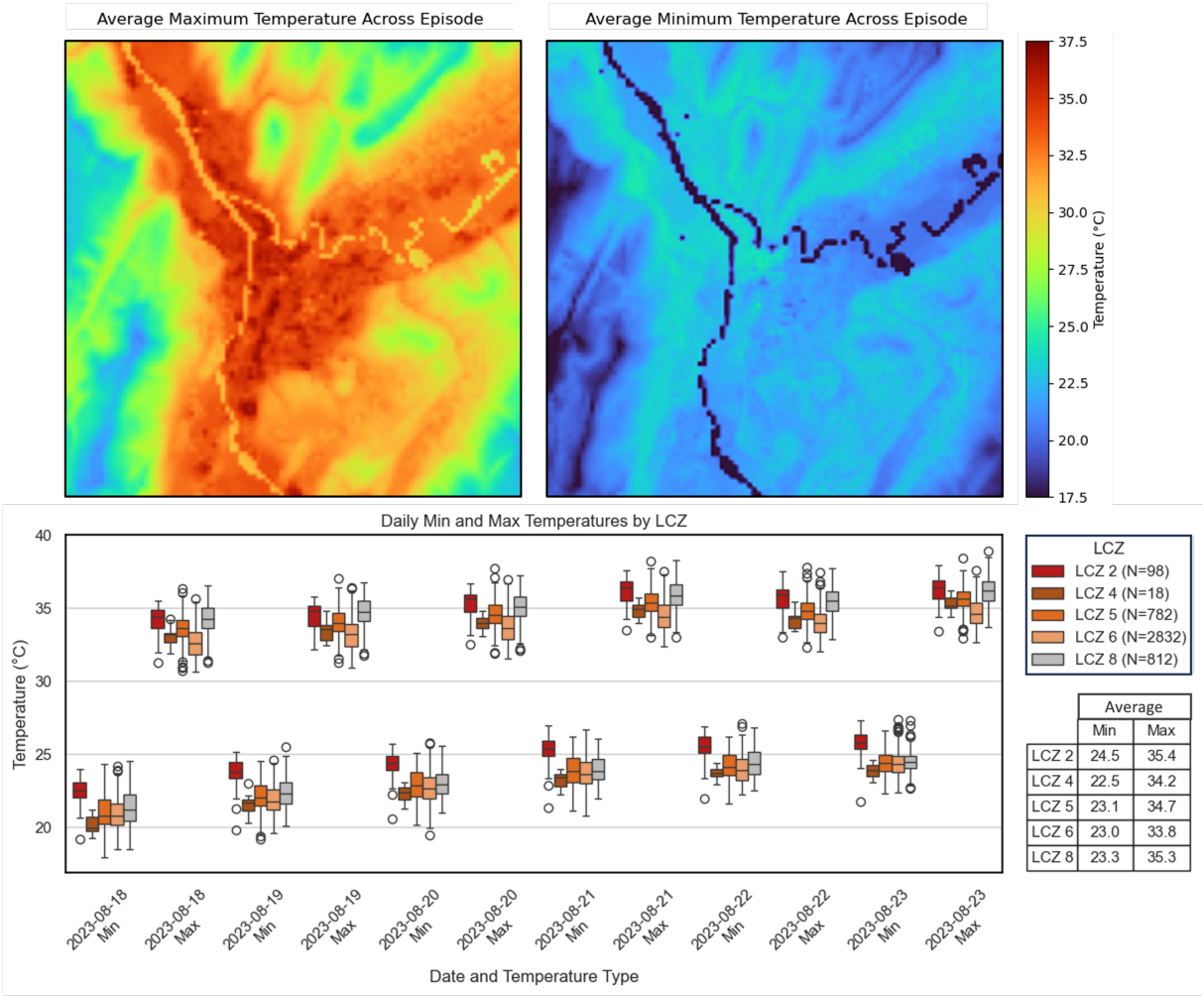

Figure 3: Overview of the control run near-surface temperature (T2) during the heatwave episode. (Top row) Spatial distribution of the average maximum (left) and average minimum (right) near-surface temperatures across the heatwave episode, overlaid with white contour lines indicating elevation at 300 m interval. (Bottom row) Box-and-whisker plots of daily minimum and maximum 2 m temperatures for each day of the episode, separated by Local Climate Zone (LCZ). Only five LCZs (2, 4, 5, 6, 8) are present in the domain. The table on the bottom right summarizes the overall average minimum and maximum temperatures for each LCZ.

The model the results were validated on its ability to replicate Grenoble's urban temperature distribution and UHI effects. Validation was conducted using data from 160 densely placed metropolitan weather stations. The model effectively simulated UHI distribution with temperature differences between urban and rural areas ranging from 3 to 5°C. However, a diurnal bias was noted. The simulation overestimates minimum nighttime temperatures by an average of 2°C and underestimates maximum daytime temperatures by an average of 4°C. This bias is a

recognized challenge in urban climate modeling (Daniel et al., 2019), often due to the complexities of diurnal temperature variation. This is specially challenging during extreme events and over complex terrain (Burger et al., 2022; Ibsen et al., 2022). However, the model's accuracy in replicating spatial temperature distribution and overall temperature patterns make it suitable for evaluating adaptation scenarios. Furthermore, this study focuses on relative changes in maximum and minimum temperature reductions for the adaptation scenarios. By comparing the control run with these scenarios, the results provide a robust framework for assessing the statistical reductions in daytime and nighttime temperatures, allowing for evaluation of the relative efficacy of the adaptation strategies.

5 Results on Individual Scenarios

This section evaluates the impacts of eight adaptation scenarios during the 2023 Grenoble heatwave, focusing on their effectiveness in reducing temperatures, improving thermal comfort (Section 5.1), and decreasing cooling energy demand (Section 6.4).

5.1 Temperature and UTCI Reductions

This section evaluates the impacts of the eight adaptation scenarios on near-surface air temperature and outdoor thermal comfort during the 2023 Grenoble heatwave. The analysis considers daytime and nighttime changes in temperature and UTCI, highlighting localized effects, trends over the heatwave, and differences in the mechanisms driving each scenario's impact.

5.1.1 Temperature and UTCI Reductions: Overall Behavior

The analysis in this section is supported by Figures 4, 5, and 6, which illustrate the trends in temperature and UTCI reductions across different adaptation scenarios. Throughout the analysis, median temperature reductions will be referred to as "median", while the 10th percentile with most reduction (P10) will be described as the "largest" reduction.

AC37: Gradual Cooling Over Time and Nighttime Improvement. The AC37 scenario shows a progressive cooling trend, particularly during nighttime. Median daytime temperature reductions are modest (-0.20°C), with reductions up to -1.3°C, mainly in the later stages of the heatwave. At night, cooling intensifies, with median reductions of -0.51°C and largest drops below -1.5°C (see Figure 4 left column). UTCI reductions follow a similar pattern (see Figure 4 right column), with stronger nighttime improvements (median: -0.28°C; largest: -1.3°C) than during the day (median: -0.11°C). These results highlight the cumulative effect of reduced air conditioning consumption in improving nighttime outside air temperature.

ALB06: Consistent Daytime Cooling and Radiation-Driven Impact. The ALB06 scenario demonstrates stable daytime cooling driven by its radiation-based mechanism. Median daytime temperature reductions reach -0.39°C, with localized drops exceeding -0.86°C, while nighttime reductions are less pronounced (median: -0.23°C). The UTCI impact aligns with this pattern, with stronger daytime reductions (median: -0.21°C; largest: -0.68°C) reflecting the scenario's focus on reducing solar radiation, though its effect on thermal comfort remains limited.

GR50: Limited Cooling and Minimal Thermal Comfort Impact. Green roofs (GR50) exhibit limited cooling effects and even warming during nighttime. Daytime temperature reductions are modest (median: -0.08°C; p10 and p90: -0.41°C to +0.25°C), and UTCI improvements are negligible (median: -0.01°C), with localized warming up to +0.33°C. At night, GR50 shows minor temperature increases (median: +0.04°C) and a marginal positive UTCI impact (+0.05°C). This is in accordance with existing literature where green roofs are expected to have notable impact on indoor temperatures and energy consumption but minor impact on city-wide outside temperatures (Salamanca et al., 2016; Zonato et al., 2021).

IsoBuild70: Day-Night Contrast in Performance. IsoBuild70 showcases contrasting impacts during the day and night. Daytime temperature changes range from -0.6°C to +0.55°C (median: +0.02°C), occasionally increasing UTCI values due to reduced heat retention and heat release into the air. At night, significant cooling is observed, with median temperature and UTCI reductions of -0.50°C and drops down to -1.25°C and -0.93°C, respectively. These results emphasize its effectiveness in addressing nighttime retained heat.

PermGround30: Modest and Localized Cooling. The PermGround30 scenario shows slight cooling effects. Median temperature reductions during the day and night are -0.16°C and -0.15°C, respectively, with UTCI reductions of -0.15°C during the day and -0.24°C at night. Largest cooling reaches -0.58°C for temperature and -0.60°C for UTCI, reflecting the scenario's limited and localized impact.

SP50: Negligible Cooling and UTCI Impact. Solar panel installations (SP50) have minimal overall impact. Daytime temperature reductions are negligible (median: -0.06°C; largest: -0.32°C), and nighttime effects are slightly stronger (median: -0.17°C; largest: -0.70°C). Similarly, UTCI reductions are minimal, with daytime and nighttime medians of -0.04°C and -0.11°C, respectively, highlighting the scenario's limited influence on thermal comfort.

TREES40: Consistent and Strong Cooling. TREES40 delivers significant and consistent cooling effects. Daytime median mean temperature reductions reach -0.52°C, with largest cooling up to -1°C, and UTCI reductions are even stronger (median: -1.0°C; largest: -1.8°C). Nighttime cooling is less pronounced but still notable, with temperature and UTCI medians of -0.32°C and -0.5°C, respectively. This is expected, as trees primarily cool through shade, which happens during the day, and it is most noticeable on UTCI. At night, cooling is limited by urban heat storage and radiation dynamics.

WetGround: Early Cooling with Diminishing Returns. The WetGround scenario shows strong initial cooling that diminishes as ground moisture decreases. Mean daytime temperature reductions start at -0.35°C (median) with largest effects reaching -1°C, but these effects weaken over time, with nighttime medians reaching only -0.11°C. UTCI reductions follow a similar pattern, with daytime medians of -0.14°C and largest drops of -0.92°C, highlighting the scenario's dependency on sustained moisture availability.

By combining these analyses, the results reveal complementary strengths across scenarios. Green strategies, such as TREES40 and ALB06, excel at daytime cooling and thermal comfort improvements, while gray strategies like IsoBuild70 and AC37 address nighttime conditions more effectively. Localized strategies, including WetGround and PermGround30, provide moderate impacts, while SP50 and GR50 exhibit limited influence. These findings suggest that a tailored

combination of green and gray strategies is essential for addressing the diverse thermal challenges of urban heatwaves.

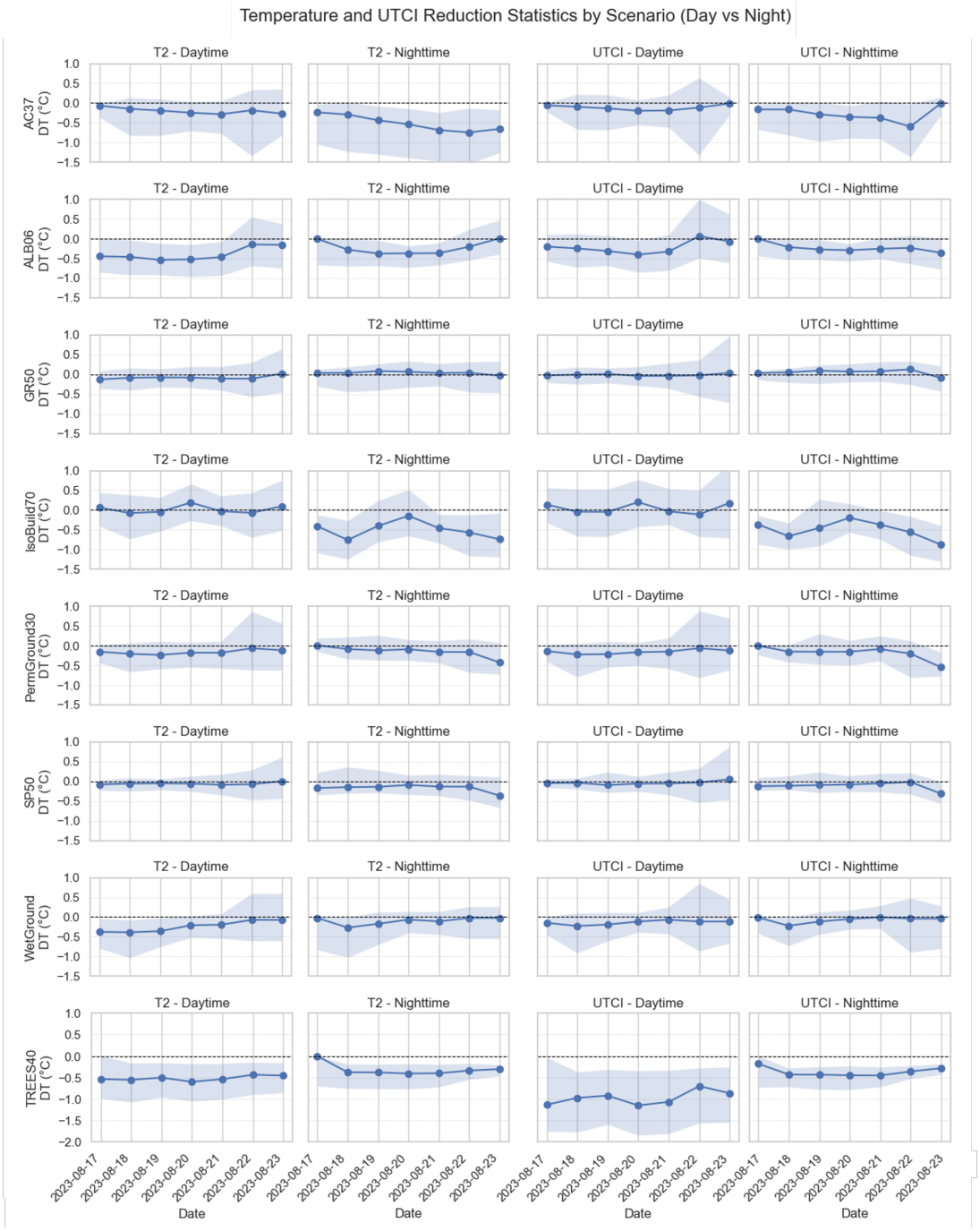

Figure 4: Temporal evolution of daytime (left) and nighttime (right) near-surface temperature and UTCI differences between each adaptation scenario and the control run during the 2023 Grenoble heatwave. Each row corresponds to a specific scenario, with blue lines representing the median temperature and UTCI change and shaded regions indicating the 10th to 90th percentile range (P10-P90). The values are computed for the urban area (all grid cells with urban local climate zone. The daytime and nighttime times are the times between sunrise and sunset and vice-versa.)

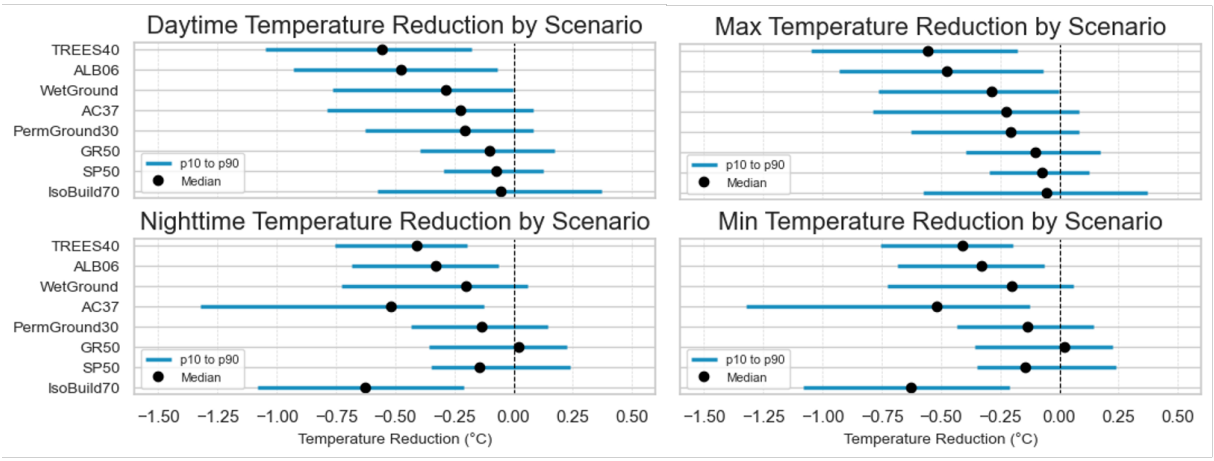

Figure 5: Daytime and nighttime temperature reductions (left), alongside maximum and minimum temperature reductions (right), for each adaptation scenario during the 2023 Grenoble heatwave. The bars represent the range from the 10th percentile (P10) to the 90th percentile (P90), and the black dots indicate the median values.

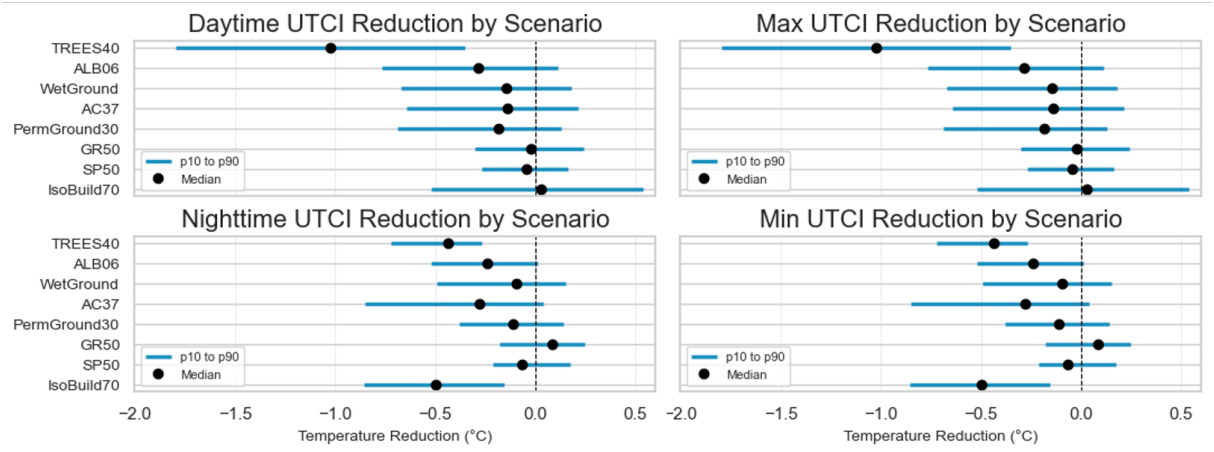

Figure 6: Same as Figure 5, but for UTCI.

5.1.2 Impact on Relative Exposure

Figure 7 summarizes how each scenario redistributes the relative exposure to different UTCI stress categories (9–26°C, 26–32°C, 32–38°C, 38–46°C, and >46°C). These percentages were obtained by aggregating the exposure over all urban grid cells and normalizing the counts within each stress range. Notably, none of the scenarios, including the Control run, show any exposure above 46°C. However, clear differences emerge in how each intervention shifts the balance between comfortable and higher-stress ranges. In the Control scenario, the comfortable UTCI range (9–26°C) accounts for 30.0% of exposure, while very strong heat stress (38–46°C) comprises 4.8%. Under the IsoBuild70 scenario, the share of exposure to very strong heat stress increases slightly to 5.7%. This indicates that while isolative building materials reduce the amount of heat stored during cooler periods, they may also lead to higher daytime maximum temperatures, since less heat is absorbed and more is transferred directly to the air. At the same time, the reduction in heat storage contributes to cooler nighttime conditions, which is reflected in the increase of the comfortable range to 32.5%. In contrast, the PermGround30 scenario re-

duces exposure in the 38–46°C range to 3.6%, indicating that enhanced ground permeability can promote cooling. Most notably, the TREES40 scenario shifts the exposure profile by reducing very strong heat stress to 0.5% and increasing the comfortable range to 33.7%.

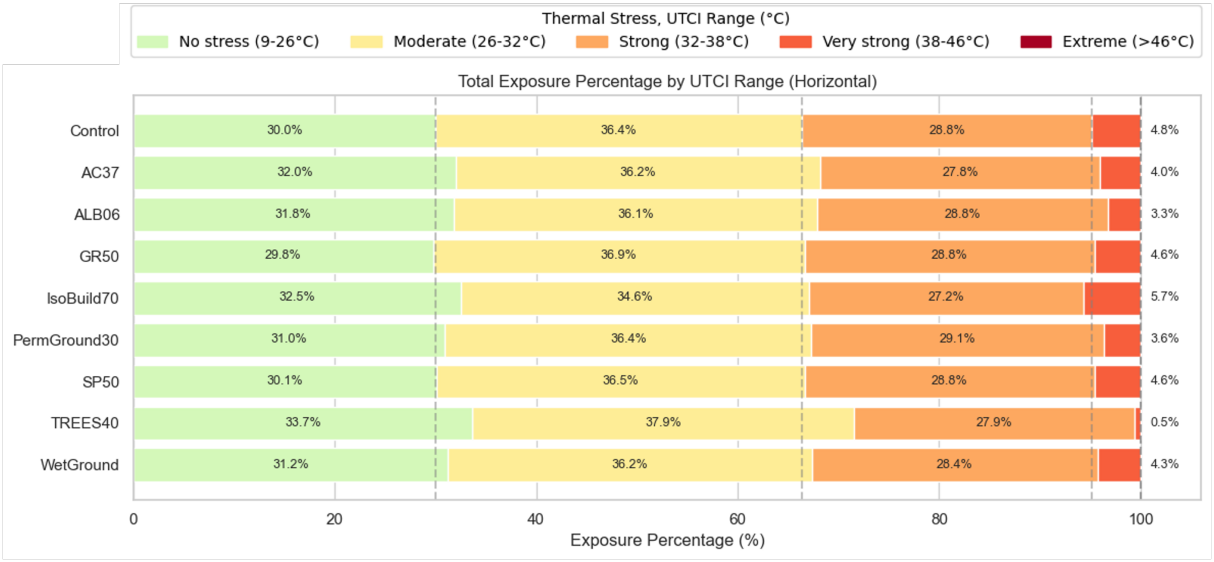

Figure 7: Percentage of exposure across UTCI ranges for each scenario during the 2023 Grenoble heatwave. TREES40 achieves the most significant reductions in very high heat stress (38-46°C), while IsoBuild70 slightly increases exposure in this range due to elevated maximum daytime values.

5.1.3 Temperature Reductions: Overall Behavior

Figures 8 and 9 illustrate the temperature differences between each adaptation scenario and the Control run for daytime and nighttime conditions, respectively. These maps reveal that the spatial structure of temperature reductions is strongly dependent on the intervention. In some scenarios the impact is more pronounced during the day than at night, while in others the reverse is true. For instance, the AC37 scenario exhibits a widespread daytime cooling effect, particularly evident around the city center, yet its nighttime impact appears more intense and localized. In contrast, the IsoBuild70 scenario shows a generally distributed cooling effect that is almost exclusively noticeable at night, with the greatest reductions concentrated in the city center (LCZ 2).

The Albedo scenario demonstrates a marked daytime effect that is most prominent near the city center, while its nighttime impact is less intense and more evenly spread across urban areas. The Trees scenario is particularly interesting; its daytime cooling follows the urban structure in terms of local climate zones and is most effective in areas with high urban fraction and available space (large low rise), hinting at a strong association with less vegetated zones, while at night its overall effect remains widespread. Scenarios such as Permeable Ground and Wet Ground produce more modest reductions: the former yields a mild and relatively uniform daytime cooling around the city center, whereas the latter shows a localized daytime impact in the center of the Y-shaped valley of Grenoble and maintains a persistent nighttime effect in areas coinciding with the city's relatively more vegetated spaces.

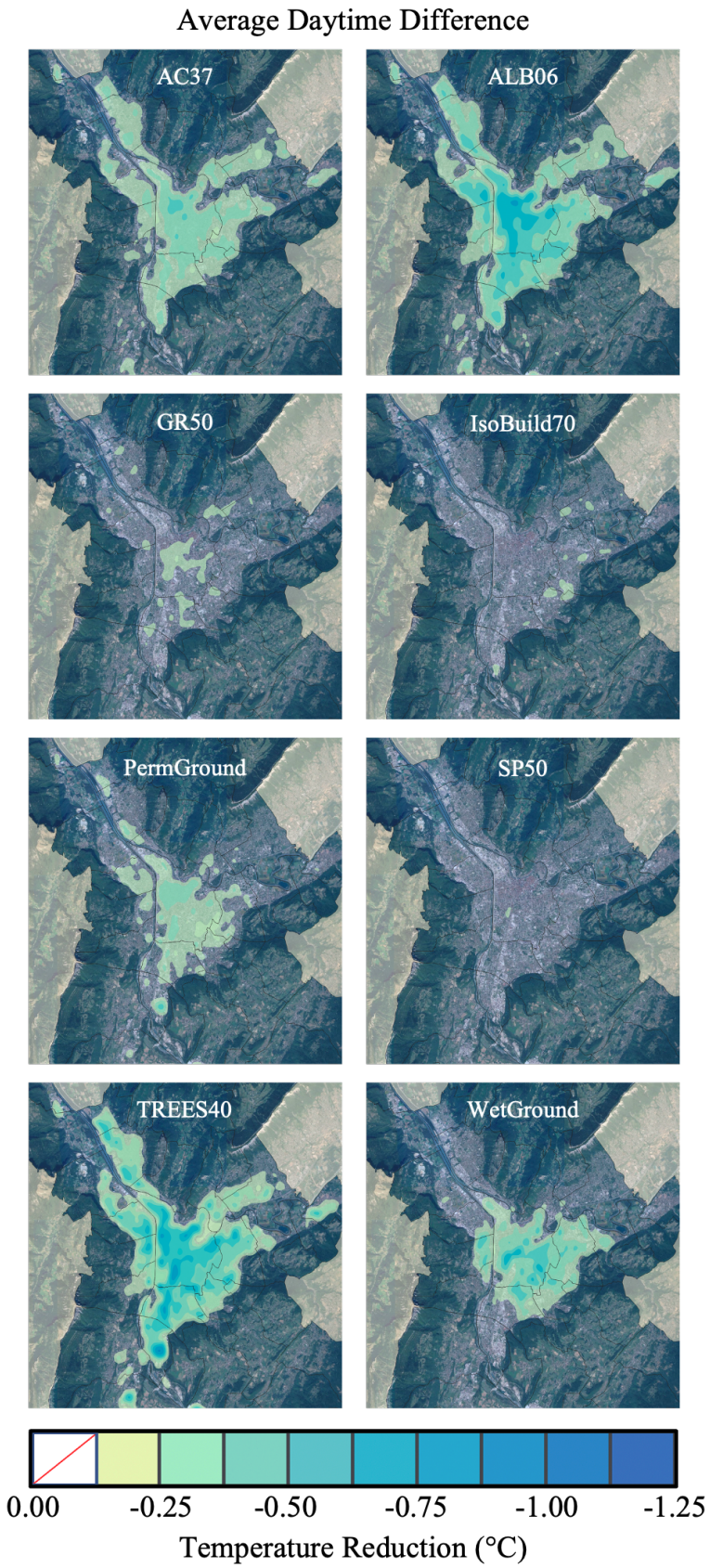

Figure 8: Spatial distribution of median daytime near-surface temperature reductions for each adaptation scenario, averaged for the entire episode.

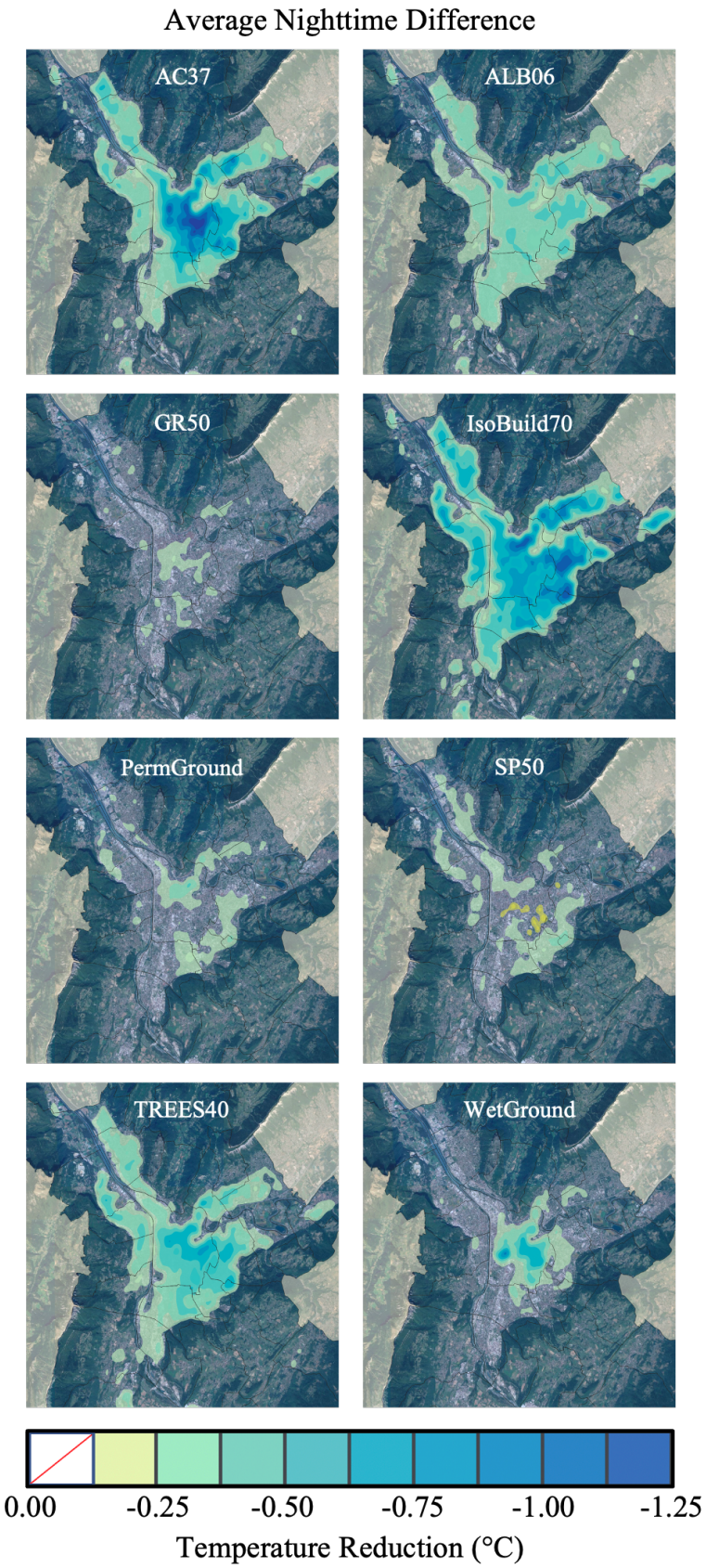

Figure 9: Spatial distribution of median nighttime near-surface temperature reductions for each adaptation scenario, averaged for the entire episode.

5.2 Energy Consumption Due to Air Conditioning

Heatwaves significantly increase energy demand, primarily due to the extensive use of air conditioning (AC) to mitigate indoor thermal discomfort. This demand exacerbates urban heat islands through waste heat emissions, creates daily power demand peaks, and places significant strain on energy infrastructure. This section evaluates the energy consumption impacts of the eight adaptation scenarios during the 2023 Grenoble heatwave, focusing on average savings, peak reductions, and cumulative benefits (see Figure 10). The control run revealed a total consumption of 80.6 GWh for the entire Metropolis daily peaks of 0.45 GW in average.

The AC37 scenario stands out as the most effective, reducing energy consumption by 64% and cutting peak demand by 290 MW (also 64%). With substantial cumulative savings of 51.74 GWh. ALB06 demonstrates moderate benefits, reducing energy use by 23% with peak reductions of 70 MW (16%). Similarly, TREES40 achieves consistent reductions of 26% of total consumption and 18% reductions of peaks loads. The last two strategies underscore the importance of addressing solar-driven heat loads. Building insulation (IsoBuild70) offers strong performance, reducing energy demand by 31% on average and cutting peaks by 140 MW (31 %), highlighting the effectiveness of a strategy directly addressing the energy efficiency of buildings.

Strategies, such as GR50, PermGround30, and SP50, show limited citywide impact. For example, green roofs (GR50) achieve an average energy savings of 9%, and permeable ground surfaces (PermGround30) provide negligible reductions. Solar panels (SP50), while offering modest shading benefits, primarily contribute to renewable energy generation rather than direct cooling impacts. Lastly the WetGround scenario demonstrates mixed results, with negligible savings and occasional increases in AC demand, possibly due to increased humidity.

In summary, strategies like AC37 and IsoBuild70 deliver the most substantial energy savings by directly addressing heat emissions and improving insulation, respectively. TREES40 and ALB06 offer moderate benefits and additional co-benefits like outdoor cooling. However, ground-based strategies show limited effectiveness in reducing citywide energy demand. These findings emphasize the need for integrated strategies to maximize cooling potential and energy efficiency in urban environments.

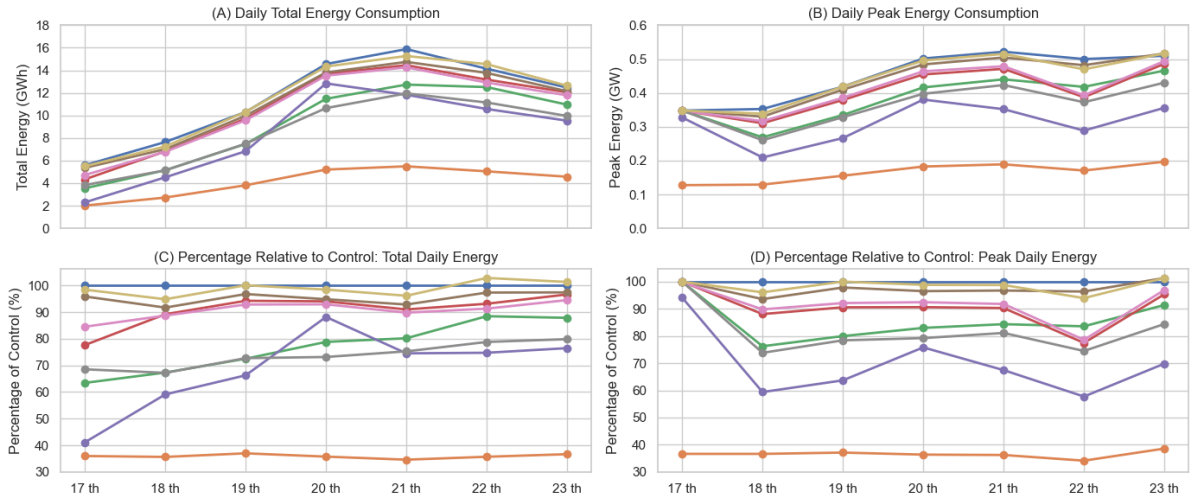

Figure 10: Comparative analysis of energy consumption and relative performance across scenarios during the heatwave event from August 17 to August 23, 2023.

6 Results: Combined Adaptation Scenarios

Individual adaptation strategies provide important benefits, but their limitations make it necessary to combine them. By integrating complementary approaches, combined scenarios can address multiple aspects of urban heat mitigation more effectively. This section explores three cumulative combinations of adaptation scenarios designed to maximize cooling impacts, improve thermal comfort, and reduce energy demand. The design of these combinations was informed by the logical interplay of strategies analysed in the previous section, with the input from local authorities and urban planners in the Grenoble Metropole, ensuring their relevance to local challenges and priorities.

The first combination of scenarios, COMB1, integrates TREES40 and IsoBuild70, leveraging their complementary strengths. TREES40 provides significant daytime cooling through shading, reducing outdoor temperatures and improving thermal comfort. IsoBuild70 enhances nighttime conditions by limiting heat transfer in buildings, reducing retained heat, and lowering energy demand. Together, these strategies address both solar-driven daytime heat and nighttime heat retention, forming a strong foundation for urban heat mitigation.

The second combination of scenarios, COMB2, builds upon COMB1 by adding ALB06. Reflective roofs in ALB06 further enhance daytime cooling by reducing solar heat absorption. This addition strengthens the daytime performance of COMB1, creating a more robust and scalable approach to reducing urban heat during peak temperatures.

The third combination of scenarios, COMB3, incorporates PermGround30 into COMB2, targeting localized cooling in urban hotspots. By replacing impermeable surfaces with permeable, vegetated ones, PermGround30 reduces heat storage and promotes evaporative cooling in streets and plazas. Its inclusion ensures that areas not directly impacted by tree shading or reflective roofs also benefit from reduced heat stress, creating a more uniform cooling effect across the urban landscape.

The progression of these combinations, summarized in Table 1 reflects a strategic approach to urban cooling, prioritizing high-impact interventions (TREES40 and IsoBuild70) while incrementally adding measures to enhance cooling and address specific urban spaces (ALB06 and PermGround30). Their design aligns with the insights from local stakeholders, ensuring these combinations are practical for implementation in Grenoble's urban environment.

Table 1: Cumulative combinations of adaptation scenarios.

COMB1 = TREES40 + IsoBuild70
COMB2 = TREES40 + IsoBuild70 + ALB06
COMB3 = TREES40 + IsoBuild70 + ALB06 + PermGround30

6.1 Temperature and UTCI Reductions

In this section, the effect of the three combined scenarios on temperature and UTCI during daytime and nighttime are discussed.

6.1.1 Overall Behavior of Temperature and UTCI Reductions

The analylis in this section is supported by the figures 11, 12 and 13. The combined adaptation scenarios demonstrate progressively stronger cooling effects across both near-surface air temperature and UTCI. These synergies are evident during both daytime and nighttime, with increasingly impactful results as additional strategies are integrated.

COMB1: Cooling with Complementary Day-Night Impacts COMB1 achieves median daytime temperature reductions of -0.5°C and UTCI reductions of -0.7°C, with largest drops (p10) reaching -1.3°C and -1.5°C, respectively (Figure 11). At night, median cooling increases to -0.7°C for temperature and -0.5°C for UTCI, with largest drops exceeding -1.5°C. These results reflect the complementary mechanisms of TREES40, which mitigates daytime heat through shading, and IsoBuild70, which reduces nighttime heat retention. The total exposure on the no-stress UTCI range is augmented more than in any individual scenario, from 30% to 36.7% (see Figure 13). Compared to the scenario of trees alone (TREE40) this scenario is not as effective in reducing the heat exposure of the very strong UTCI range (0.9% as opposed to 0.5% of exposure). This is because of the counteracting effect of the building insulation measures which, as seen in previous sections, can slightly exacerbate maximum temperatures. It is however an effective compromise.

COMB2: Amplified Daytime Cooling Adding ALB06 to COMB1 in COMB2 enhances median daytime temperature reductions to -1.3°C and UTCI reductions to -1.6°C . Largest effects exceed -2.0°C for both metrics (Figure 11). Nighttime reductions are also notable, with median values of -1.6°C for temperature and -1.3°C for UTCI. The reflective roofs of ALB06 amplify daytime cooling by reducing solar heat absorption, complementing the effects of TREES40 and IsoBuild70. Compared to COMB1, this scenario further reduces the exposure in the strong and very strong ranges of UTCI from 28.6% to 25.8%, while augmenting the exposure in the comfortable range to 38%.

COMB3: Maximized Cooling Across All Metrics COMB3, which incorporates PermGround30, achieves the strongest results. Median temperature reductions reach -1.7°C during both day and night, while UTCI reductions are -1.9°C during the day and -1.7°C at night. Largest effects approach -2.5°C for both metrics. The addition of PermGround30 enhances evaporative cooling, particularly in areas with high impermeable surface coverage. These cumulative benefits significantly reduce exposure to extreme heat stress, with COMB3 lowering exposure to high UTCI conditions ($38-46$°C) from 4.8% in the baseline to 0.1%, while increasing exposure to low-stress conditions ($9-26$°C) to 39.1%. Compared to COMB2, this scenario further reduces the exposure in the strong and very strong ranges of UTCI from 25.8% to 24.8%, while augmenting the exposure in the comfortable range to 39.1%.

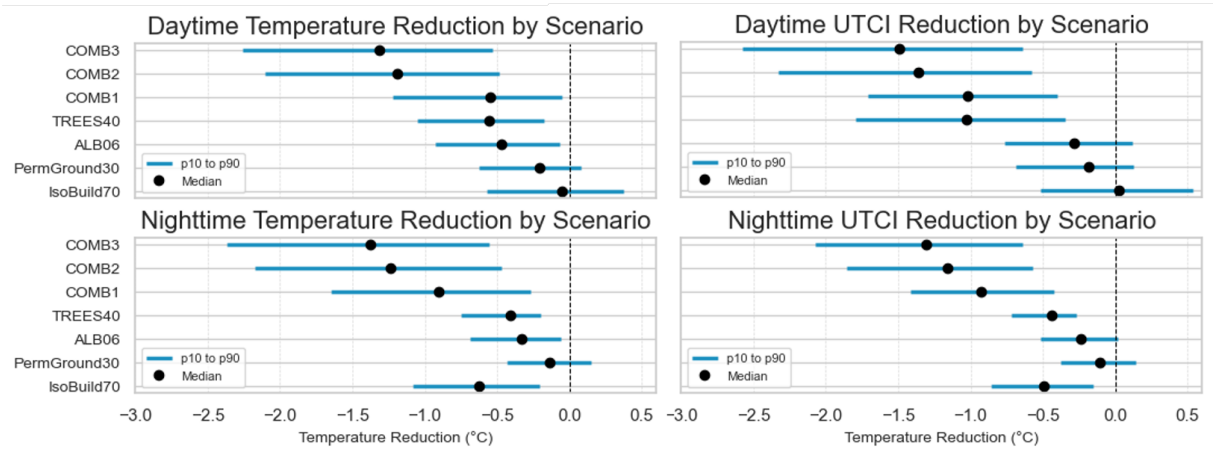

Figure 11: Daytime and nighttime temperature reductions (left), alongside UTCI reductions (right), for the four individual adaptation scenarios and the combined scenarios. Represented as in Figure 5.

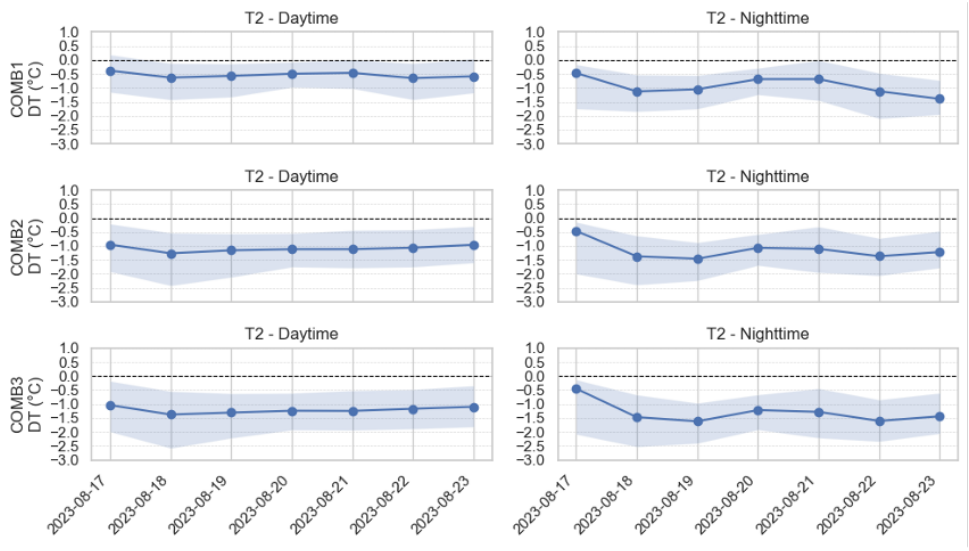

Figure 12: Temporal evolution of daytime (left) and nighttime (right) near-surface air temperature (T2) differences between the combined scenario and the control run during the 2023 Grenoble heatwave. Each row corresponds to a specific scenario, with blue lines representing the median temperature reduction and shaded regions indicating the 10th to 90th percentile range (P10-P90).

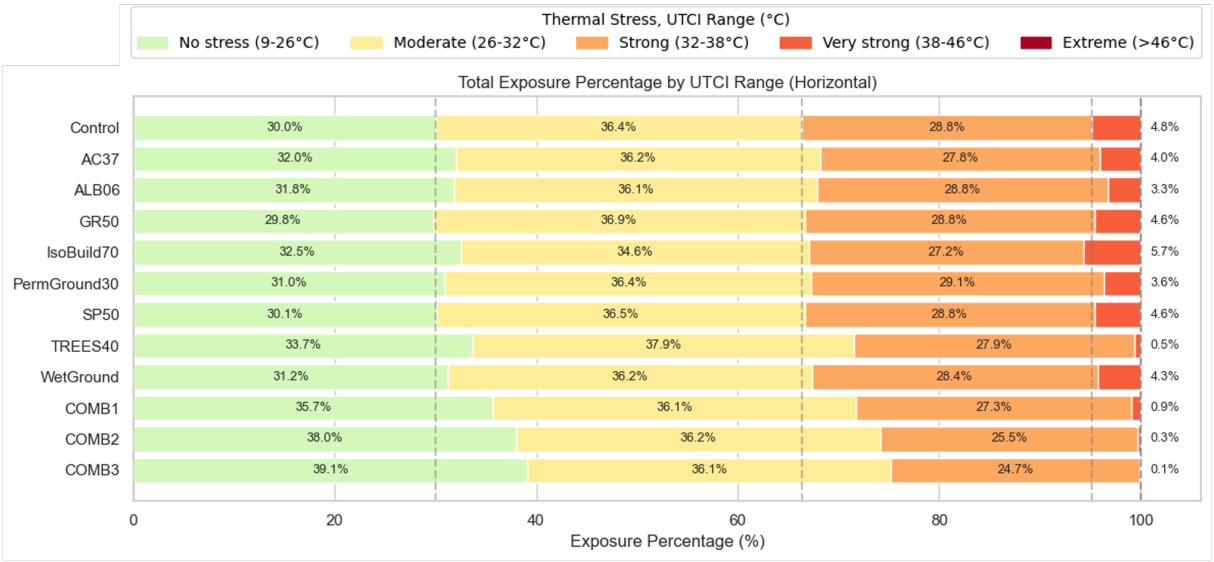

Figure 13: Percentage of exposure across UTCI ranges for each scenario, including the combination scenarios during the 2023 Grenoble heatwave.

6.1.2 Spatial Distribution of Temperature and UTCI Reductions

Figures 14 and 15 depict how the combined scenarios modify daytime and nighttime near-surface temperature and UTCI relative to the Control run. Notably, these maps often resemble a superimposed effect of their constituent single-strategy measures. For instance, during the day, COMB1 shows cooling patterns similar to those from the TREES40 intervention, whereas at night, its spatial distribution echoes IsoBuild70. This reflects how the combined scenario resembles each individual measure at its most effective time of day. In general, all combined

scenarios yield broader and more consistent cooling than any single intervention, indicating that bundling strategies with distinct diurnal strengths can enhance both daytime and nighttime mitigation of heat stress.

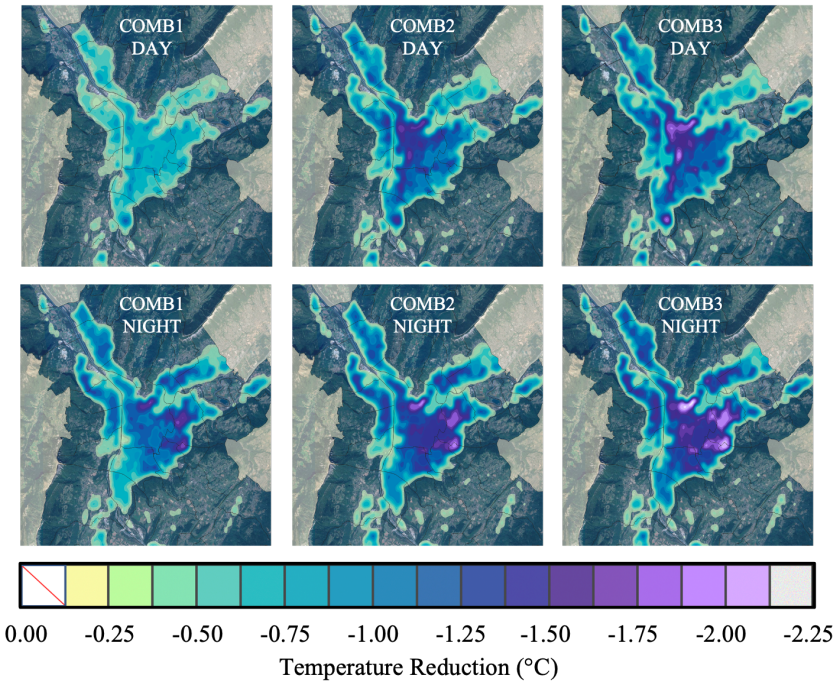

Figure 14: Spatial distribution of median daytime and nighttime near-surface temperature reductions for each combined scenario during the 2023 Grenoble heatwave.

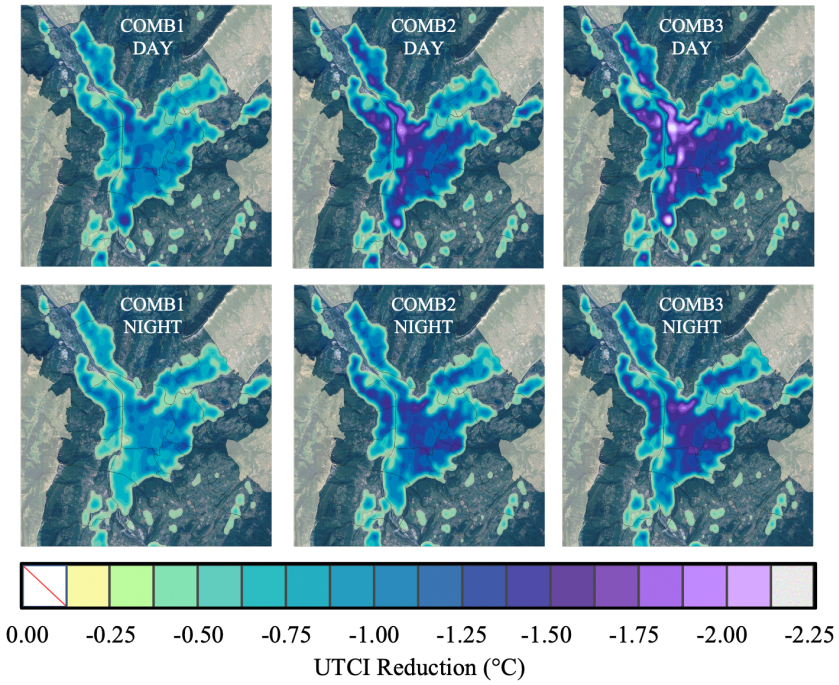

Figure 15: Spatial distribution of median daytime and nighttime UTCI reductions for each combined scenario during the 2023 Grenoble heatwave.

6.2 Temperature Reduction in Relation to Urbanization

This section examines how temperature reductions achieved by adaptation strategies vary with specific urban parameters. The urban fabric can be described with many different parameters. One example is the sky view factor which typically correlates with the urban heat island effect. Here however we will focus on those parameters that form the urban-specific input of the model. These include urban fraction (the fraction of each grid cell covered by construction), building area fraction (the ratio of building footprint area to the grid cell area), total building surface fraction (the fraction of total building surface compared to the grid cell area), mean building height (the building height average weighted with building area fraction) and the Local Climate Zones. The results are displayed in Figure 16.

A key trend across all adaptation scenarios is the increasing temperature reduction observed with higher urban density (16 A, B, C). These densely built environments, characterized by a larger thermal inertia and lower albedo, experience heightened baseline temperatures, making them more receptive to cooling strategies. Scenarios such as IsoBuild70, which focuses on improving building insulation, and TREES40, which increases vegetation coverage, deliver notable temperature reductions in these areas. Combined strategies, achieve the greatest impacts, exceeding 1°C reductions in densely urbanized zones.

In contrast, the relationship with building height demonstrates a non-linear pattern (16 D). While mid-rise buildings (12–18 m) show the most substantial reductions, areas with taller structures (>18 m) exhibit diminished gains. The interplay that causes this behavior can be very complex. A possible reason for this is due to increased solar exposure, reduced shading, and the limited effectiveness of ground-based cooling measures in these contexts. Strategies targeting rooftops, such as ALB06 (high-albedo roofs), remain effective but are less impactful compared to those aimed at urban materials or vegetation enhancements.

Analysis of reductions per Local Climate Zones (LCZs) provides further insight into these dynamics (16 D). Cooling effects are most pronounced in LCZ 2 (compact mid-rise), LCZ 5 (open mid-rise), LCZ 8 (industrial low-rise), and LCZ 4 (open high-rise), with LCZ 6 (open low-rise) showing the least reduction. The TREES40 scenario is particularly effective in LCZs 2, 4, and 5, where dense urban fabric or limited vegetation makes tree planting a significant intervention. However, in LCZ 6, where vegetation is already abundant, the marginal impact of additional trees is smaller. Interestingly, LCZ 8 (industrial zones) experiences substantial cooling under TREES40, likely due to the predominance of impervious surfaces and construction materials that amplify the benefits of added vegetation.

Conversely, the IsoBuild70 scenario is more effective in LCZs associated with larger building surface fraction, such as LCZ 2, LCZ 5. Its effectiveness is reduced in LCZs 4 and 6, where smaller building surface fraction and greater vegetative cover limit the impact of insulation strategies. These results underscore the need to tailor adaptation measures to the specific characteristics of urban zones to maximize their effectiveness.

Overall, temperature reductions are strongly mediated by urban parameters such as density, surface coverage, and building height, as well as the classification of Local Climate Zones. Densely built environments with limited vegetation, mid-rise buildings, and compact urban forms offer the greatest potential for impactful cooling interventions. These results emphasize the critical role of urban morphology in determining the effectiveness of adaptation measures and highlight the need for tailored strategies that align with the unique characteristics of each urban environment.

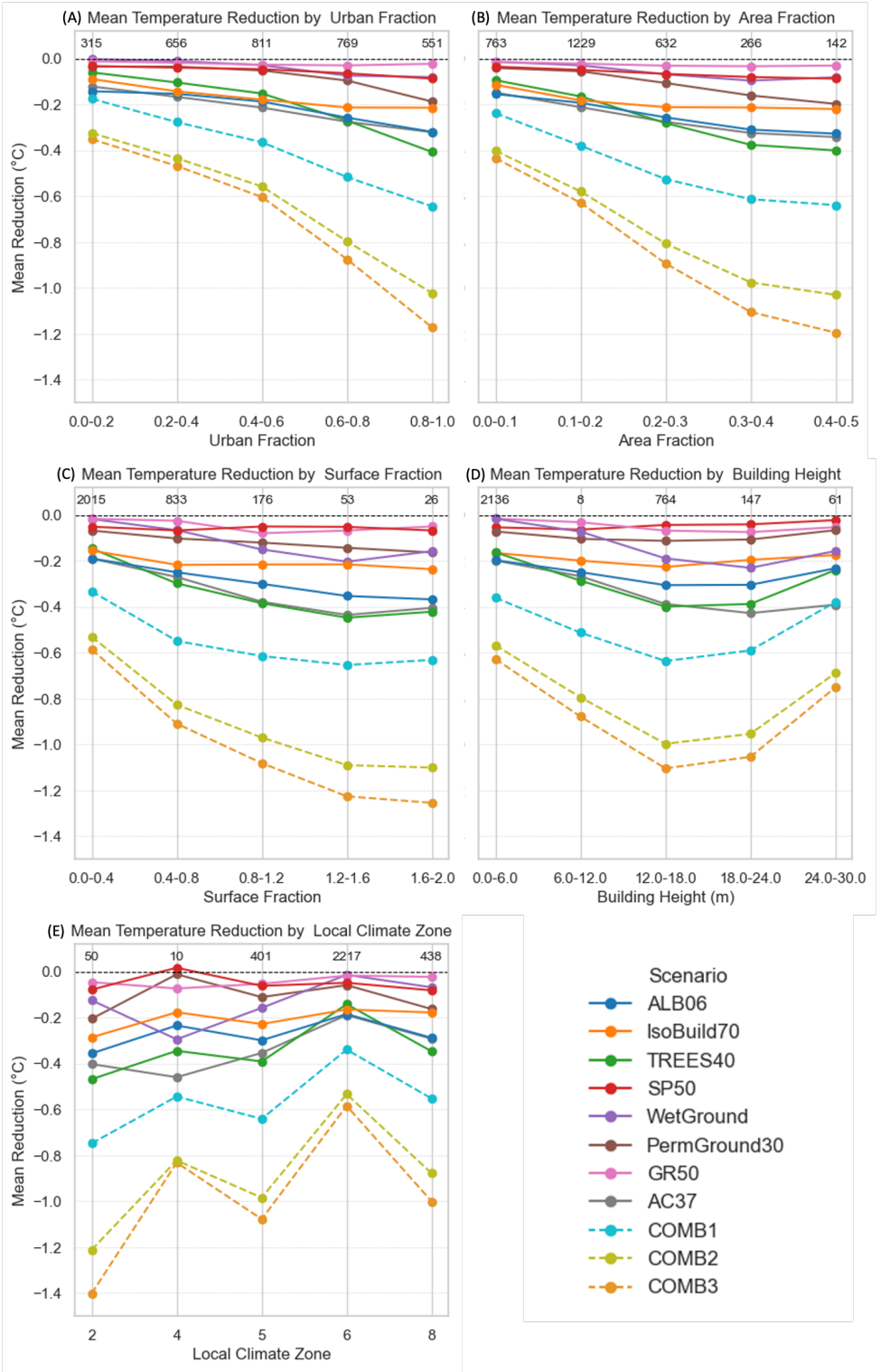

Figure 16: Mean temperature reductions (°C) across urban parameter categories under different adaptation scenarios. The panels illustrate reductions by urban fraction, area fraction, surface fraction, building height, and Local Climate Zone (LCZ).

6.3 Interaction of Cumulative Effects

The analysis of cumulative effects in the combined scenarios (COMB1, COMB2, and COMB3), is displayed in Figure 17. This figure reveals a strong linear relationship between the temperature reductions of the combined strategies and the additive contributions of their individual components. This relationship is more linear during the day ($R^2 > 0.98$) but still notable during the night ($R^2 > 0.95$).

The linear fit suggests a slight compound effect during the day, particularly in COMB2, where the slope of the linear fit exceeds 1 (1.08). This indicates that the combined daytime effect of TREES40, IsoBuild70, and ALB06 slightly exceeds the sum of their individual contributions, likely due to synergistic interactions among shading, reflective cooling, and insulation mechanisms.

Conversely, during the night, the slope of the linear fit of 0.85 or less indicates a slight underestimation of the combined effect compared to the linear summation. This suggests that the individual strategies may interact non-linearly at night, with diminishing returns from certain mechanisms (such as insulation or evaporative cooling) when combined. This result highlights the importance of considering potential interactions when modeling nighttime cooling, as combined strategies may not always yield additive results.

Overall, these findings show the utility of using individual scenario impacts as a first-order approximation for the combined effects, particularly during the day. However, they also highlight the need to account for non-linear interactions during nighttime cooling.

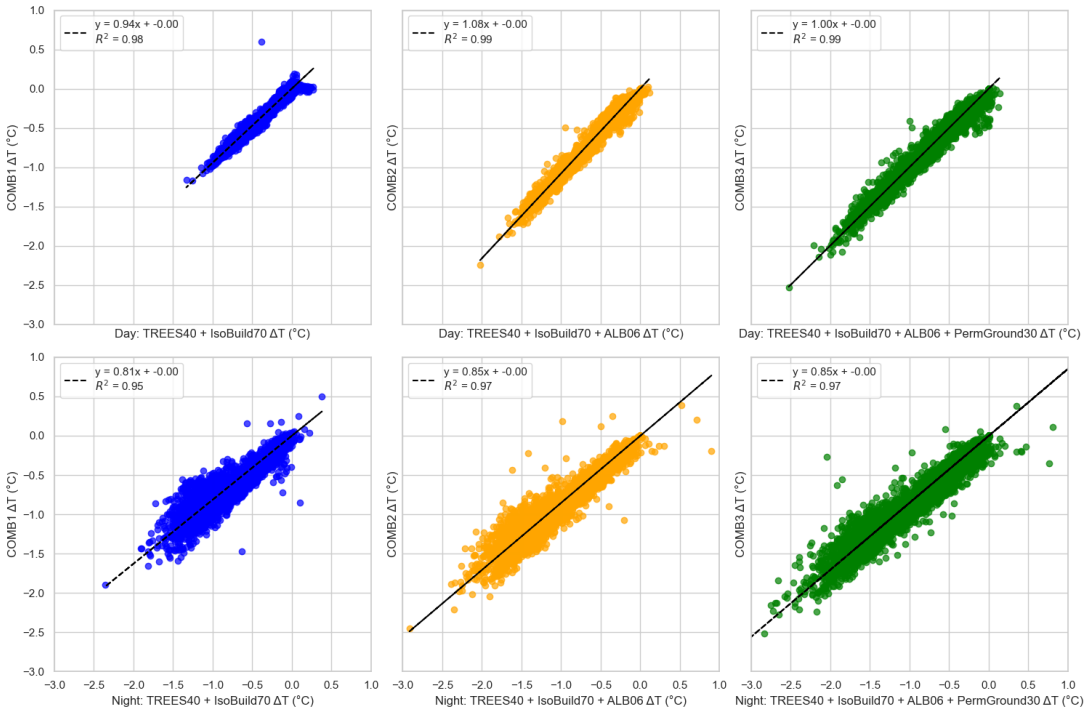

Figure 17: Scatter plots comparing temperature reductions of combined scenarios (COMB1, COMB2, and COMB3) with the addition of their respective constituent scenarios. The top row represents daytime comparisons, while the bottom row represents nighttime comparisons. Each plot shows the linear fit, equation, and R^2 value, indicating the degree to which the combined scenario aligns with the sum of its components.

6.4 Energy Consumption

The combined scenarios also exhibit significant reductions in energy consumption for air conditioning (Figure 18). COMB1 reduces total energy use by 50%, saving 36.12 GWh relative to the control. COMB2 further increases savings to 44.62 GWh, corresponding to a 60% reduction. COMB3 achieves the largest savings, reducing consumption by 46.60 GWh, a 62% reduction compared to the control.

As it is indicated in Table AT3, the combined scenarios also show notable reductions in peak energy consumption. COMB1 reduces peak demand by 0.20 GW, representing a 44% decrease compared to the control. COMB2 achieves a further reduction by 0.23 GW, a 51% decrease. COMB3 delivers the most substantial peak savings, reducing peak demand by 0.25 GW, a 55% reduction relative to the control scenario.

Importantly, no individual or combined strategy achieves energy savings below the AC37 scenario, which represents the current state of air conditioning adoption in Grenoble. This underscores the substantial energy savings potential of reducing reliance on air conditioning through urban adaptation measures. However, during extreme heat events, when outdoor temperatures can reach 40 degrees, reducing AC usage alone is not sufficient. Ensuring thermal comfort and protecting the well-being of residents, especially the most vulnerable, must remain central to any adaptation strategy.

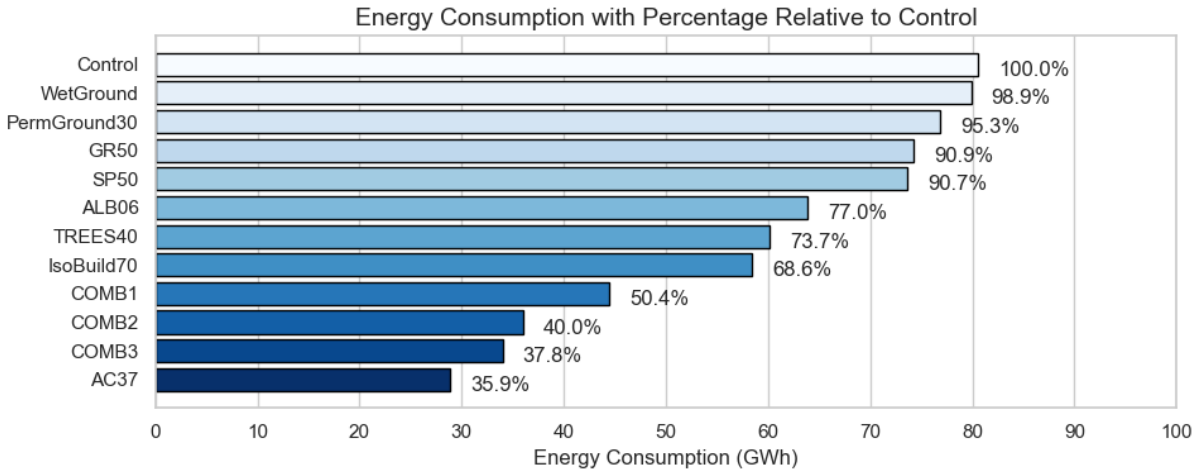

Figure 18: Energy consumption relative to the control scenario for various adaptation strategies during the 2023 Grenoble heatwave. The bars represent the total accumulated energy consumption in GWh for each scenario, expressed as a percentage of the control.

7 Energy Generation by Solar Panels (SP50)

The SP50 scenario represents a mitigation strategy where 50% of rooftops in the Grenoble metropolitan area are equipped with solar panels. The potential for energy generation from these panels was evaluated over the 2023 heatwave episode, providing insights into their performance during periods of high solar radiation. Figure 19 illustrates the temporal evolution of power production and accumulated energy generated throughout the episode.

The upper panel of Figure 19 demonstrates the diurnal cycle of power production. Peak production aligns with midday solar radiation, with maximum power outputs consistently exceeding 0.11 GW. During the night, power production drops to zero, as expected. The lower panel of Figure 19 shows the accumulation of generated energy over time, reaching a total of

approximately 19.2 GWh by the end of the heatwave episode.

The energy generated demonstrates a clear temporal trend, with slightly lower production on cloudy days, as observed on August 19th and August 22nd. However, overall, the SP50 scenario maintained a stable and predictable output pattern.

The energy generated by solar panels under the SP50 scenario corresponds to approximately 25% of the total energy consumption of the control scenario during the heatwave period (80.5 GWh). This represents a significant potential for offsetting energy demands, particularly during peak consumption hours. Notably, the alignment of peak solar generation with high air-conditioning demand further enhances the effectiveness of this mitigation strategy.

While the SP50 scenario provides substantial energy generation, its effectiveness depends on implementation feasibility. Factors such as rooftop availability, solar panel efficiency, and maintenance could influence real-world applicability. Additionally, while solar panels directly reduce energy consumption from non-renewable sources, they do not address thermal comfort or urban heat island effects. Thus, they should be considered as a complementary solution alongside other strategies.

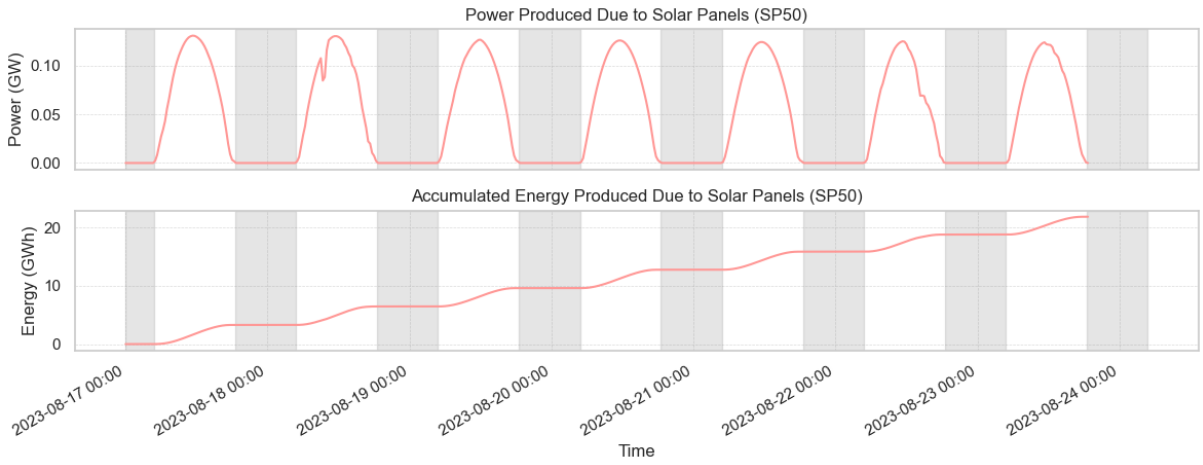

Figure 19: Power production and accumulated energy generated by solar panels (SP50) during the 2023 Grenoble heatwave. The upper panel shows the diurnal variation in power generation, with peaks exceeding 0.11 GW during midday and zero production at night. The lower panel illustrates the cumulative energy generated, totaling approximately 19.2 GWh by the end of the episode.

8 Discussion

This study provides a detailed assessment of urban heat adaptation strategies, analyzing their impacts on temperature, thermal comfort, energy consumption, and their combined effects during an extreme heatwave in Grenoble, France. The findings revealed the strengths and limitations of each strategy as well as insights into their interactions and the influence of urban characteristics on their effectiveness.

Green strategies exhibited varying levels of effectiveness in reducing temperature and improving thermal comfort. The tree-based scenario, TREES40, which increases tree coverage to provide shading and reduce thermal stress, consistently emerged as the most effective green strategy. It achieved significant reductions in both daytime and nighttime temperatures and enhances thermal comfort across urban areas. Its success is likely due to a combination of shading and reduced thermal mass exposure. PermGround30, designed to improve water infiltration

through permeable ground surfaces, is the second most effective green strategy, providing notable localized cooling, though its citywide impact remains modest. GR50, which implements green roofs to increase insulation and evaporative cooling, showed limited impact. WetGround, which saturates the ground to promote evaporative cooling, initially demonstrates strong cooling potential but experiences diminishing returns as soil moisture levels decrease. Notably, the urban tree parameterization does not account for evapotranspiration effects, which may underestimate their cooling benefits, which would mean the need for improved representation of vegetation processes in future studies.

Gray strategies, which target infrastructure and material modifications, also showed notable results. ALB06, implementing high-albedo roofs to reflect solar radiation, is particularly effective in reducing daytime temperatures by minimizing heat absorption. IsoBuild70, enhancing building insulation to reduce heat transfer, excels at mitigating nighttime heat retention, significantly improving thermal comfort during nocturnal hours. However, the daytime effects are more nuanced. By reducing the thermal exchange between buildings and the outdoor environment, the strategy prevents buildings from absorbing excess heat during the day. This can lead to a localized increase in outdoor air temperatures in dense urban areas, where heat is retained in the urban fabric instead of being partially absorbed by buildings. SP50, which represents the installation of solar panels on rooftops up to half of the total roof surface, contributes minimally to direct cooling but provides substantial benefits for renewable energy generation, offsetting nearly 25% of the energy demands caused by extreme heat with respect to the control run. These results emphasize the diverse pathways by which gray strategies can influence urban heat dynamics, with some excelling in direct temperature modulation and others providing complementary benefits.

The soft strategy, AC37, represents a reduction in air conditioning consumption to 37% of households, reflecting Grenoble's current adoption rate. In the rest of the scenarios and the control run it is assumed that 100% of the households are equipped with air conditioning. This strategy demonstrates notable temperature and thermal comfort improvements, particularly at night. The implications on temperature, thermal comfort, and energy demand highlight its potential role as part of broader adaptation measures.

Energy consumption analysis revealed a clear distinction between the impacts of different strategies. Building-focused strategies (such as IsoBuild70), together with the tree-based strategy (TREES40), yielded the most substantial reductions in energy demand due to their direct effects on indoor environments. IsoBuild70's insulation improvements effectively reduced cooling energy needs by limiting heat transfer. SP50 showed a modest impact on energy consumption of nearly 10% in savings, though showing strong indirect contribuition by offsetting nearly 25% of the energy demands through renewable energy generation. In contrast, ground-based strategies like PermGround30 and WetGround had negligible effects on energy consumption, as their benefits are primarily related to urban temperature reductions rather than direct building cooling. These findings highlight the dual role of building-based strategies in addressing both urban heat and energy demand, emphasizing their direct contribution to mitigating indoor temperature stress and reducing energy reliance. Meanwhile, the limited influence of ground-based interventions on energy systems underscores the importance of tailoring strategies to their intended scope of impact.

The combined scenarios—COMB1, COMB2, and COMB3—demonstrate the enhanced effectiveness of integrating multiple strategies. During the day, the effects of combining strategies often exhibit an almost linear addition, with some instances of compounding effects, such as the synergistic interaction between shading (TREES40), building insulation (IsoBuild70) and reflective surfaces (ALB06). At night, however, the combined effects are slightly less than additive, possibly due to overlapping mechanisms reducing their cumulative impact. This means

that individual scenario simulations represent a good first approximation of their combinations, although it is needed to simulate them together to extract their complete complex interaction. The results highlighted that while individual strategies provide important benefits, they are insufficient on their own to fully address the challenges of extreme urban heat. Combining strategies allows for more comprehensive mitigation, addressing both daytime and nighttime heat stress while reducing energy demand.

The effectiveness of the strategies appears determined by the level of urbanization. The impacts on temperature and thermal comfort are most pronounced in densely urbanized areas, where high thermal mass, low albedo, and limited vegetation exacerbate heat retention. Strategies like TREES40 and IsoBuild70 deliver the greatest benefits in these areas, reflecting their targeted approaches to urban heat mitigation. TREES40 benefits from its ability to provide shading and reduce thermal stress, particularly in areas with low vegetation and high thermal mass, while IsoBuild70's insulation improvements directly address heat retention, especially during nighttime. The scope of these measures, however, must align with the local political possibilities and interests. In this work, the city center, the area of the city most affected by the heat, is home to a number of historical buildings that are part of France historical heritage. Modifications there are most challenging, especially when it comes to modifying building exteriors.

While this study provides valuable insights, it is important to acknowledge that these findings are derived from simulations using a model. Although models are powerful tools for exploring "what-if" scenarios and predicting outcomes under varying conditions, they remain simplifications of reality. The assumptions, parameterizations, and limitations inherent to any model, including those related to vegetation processes and urban dynamics, can influence the results. This underscores the need to interpret findings with caution and to supplement modeling efforts with observational data and real-world experiments whenever possible.

9 Conclusions

This study highlights the critical role of green, gray, and soft adaptation strategies in mitigating the impacts of extreme urban heatwaves. Among green strategies, the tree-based strategy proved the most effective, significantly reducing temperatures and improving thermal comfort, with the permeable ground increase strategy offering complementary cooling benefits. Gray strategies, such as cool roof and insulation of buildings, provided targeted solutions, excelling in daytime cooling and nighttime thermal comfort, respectively. Soft strategies like AC37 showcased the potential of operational changes to complement infrastructure-based solutions.

Energy consumption analysis revealed that building-focused strategies, substantially reduced energy demand by addressing indoor cooling needs. Ground-based strategies had minimal direct impact on energy consumption but contributed indirectly through urban cooling. The scenario of increase in use of solar panels stood out for its ability to offset energy demand through renewable generation.

Combining strategies proved more effective than individual approaches, with near-linear added effects during the day and slightly diminished addition of impacts at night. This synergy underscores the importance of integrated solutions to address both daytime and nighttime heat stress while reducing energy demands.

Finally, the effectiveness of these strategies was most pronounced in densely urbanized areas, where extreme heat impacts are most severe. Tailoring interventions to local urban contexts is essential, particularly in areas with significant implementation challenges.

Although the design of the scenarios was carefully tailored in collaboration with local authorities to align with Grenoble's urban context and policy goals, this work should be viewed

as a proof of concept. Its primary purpose is to inform and provide a framework for evaluating potential interventions. To fully address the impacts of future policies, further work is needed to refine the scenarios, incorporate additional complexities of urban systems, and validate outcomes against real-world implementations. This iterative process will enhance the reliability and applicability of such studies for guiding effective urban adaptation strategies.

In conclusion, this study underscores the importance of integrated approaches to urban heat adaptation. Green, gray, and soft strategies each offer unique advantages, but their combined application delivers the most comprehensive benefits. By prioritizing multi-faceted interventions and tailoring strategies to local conditions, cities like Grenoble can effectively enhance resilience to future heatwaves, advancing both urban sustainability and climate adaptation goals.

10 Appendix Chapter

Table AT1: Temperature Reductions (Median, P10, P90) Across Scenarios

(a) Daytime Reductions

Scenario	Median	P10	P90
AC37	-0.17	-0.63	0.13
ALB06	-0.32	-0.74	0.06
GR50	-0.06	-0.34	0.16
IsoBuild70	-0.04	-0.47	0.29
PermGround30	-0.10	-0.48	0.16
SP50	-0.05	-0.26	0.13
TREES40	-0.34	-0.86	-0.03
WetGround	-0.12	-0.53	0.16
COMB1	-0.60	-1.21	-0.08
COMB2	-1.25	-2.10	-0.50
COMB3	-1.30	-2.30	-0.56

(b) Nighttime Reductions

Scenario	Median	P10	P90
AC37	-0.30	-0.94	0.05
ALB06	-0.28	-0.65	0.01
GR50	0.06	-0.19	0.25
IsoBuild70	-0.46	-0.97	-0.03
PermGround30	-0.08	-0.38	0.15
SP50	-0.11	-0.32	0.10
TREES40	-0.27	-0.61	-0.06
WetGround	-0.08	-0.43	0.18
COMB1	-0.90	-1.70	-0.25
COMB2	-1.26	-2.21	-0.50
COMB3	-1.39	-2.41	-0.57

(c) Maximum Temperature Reductions

Scenario	Median	P10	P90
AC37	-0.18	-0.50	0.07
ALB06	-0.44	-0.75	-0.12
GR50	-0.15	-0.34	0.07
IsoBuild70	0.11	-0.13	0.38
PermGround30	-0.16	-0.48	0.09
SP50	-0.09	-0.28	0.12
TREES40	-0.65	-0.98	-0.37
WetGround	-0.23	-0.59	0.02
COMB1	-1.00	-1.80	-0.40
COMB2	-1.60	-2.50	-0.75
COMB3	-1.75	-2.70	-0.85

(d) Minimum Temperature Reductions

Scenario	Median	P10	P90
AC37	-0.20	-0.46	-0.04
ALB06	-0.17	-0.33	0.01
GR50	0.12	-0.16	0.29
IsoBuild70	-0.40	-0.64	-0.07
PermGround30	-0.13	-0.27	0.04
SP50	-0.14	-0.29	0.05
TREES40	-0.22	-0.30	-0.12
WetGround	-0.08	-0.28	0.07
COMB1	-0.70	-1.20	-0.20
COMB2	-1.10	-1.70	-0.45
COMB3	-1.25	-1.90	-0.50

Median, P10, and P90 values for temperature reductions across adaptation scenarios. The results are divided into (a) daytime average reductions, (b) nighttime average reductions, (c) reductions in maximum temperatures, and (d) reductions in minimum temperatures. Combined scenarios COMB1, COMB2, and COMB3 show enhanced effectiveness.

Corine Land Cover (CLC)		United States Geological Survey (USGS)	
ID	Description	ID	Description
1.1.1	Continuous urban fabric	32	High Intensity Residential
1.1.2	Discontinuous urban fabric	31	Low Intensity Residential
1.2.1	Industrial or commercial units	33	Industrial or Commercial
1.2.2	Road and rail networks	33	Industrial or Commercial
1.2.3	Port areas	33	Industrial or Commercial
1.2.4	Airports	33	Industrial or Commercial
1.3.1	Mineral extraction sites	19	Barren or Sparsely Vegetated
1.3.2	Dump sites	19	Barren or Sparsely Vegetated
1.3.3	Construction sites	19	Barren or Sparsely Vegetated
1.4.1	Green urban areas	7	Grassland
1.4.2	Sport and leisure facilities	7	Grassland
2.1.1	Non-irrigated arable land	2	Dryland Cropland and Pasture
2.1.2	Permanently irrigated land	3	Irrigated Cropland and Pasture
2.1.3	Rice fields	3	Irrigated Cropland and Pasture
2.2.1	Vineyards	6	Cropland/Woodland Mosaic
2.2.2	Fruit trees and berry plantations	6	Cropland/Woodland Mosaic
2.2.3	Olive groves	6	Cropland/Woodland Mosaic
2.3.1	Pastures	2	Dryland Cropland and Pasture
2.4.1	Annual crops	6	Cropland/Woodland Mosaic
2.4.2	Complex cultivation patterns	4	Mixed Dryland/Irrigated Cropland
2.4.3	Agricultural land	5	Cropland/Grassland Mosaic
2.4.4	Agro-forestry areas	6	Cropland/Woodland Mosaic
3.1.1	Broad-leaved forest	11	Deciduous Broadleaf Forest
3.1.2	Coniferous forest	14	Evergreen Needleleaf Forest
3.1.3	Mixed forest	15	Mixed Forest
3.2.1	Natural grasslands	7	Grassland
3.2.2	Moors and heathland	9	Mixed Shrubland/Grassland
3.2.3	Sclerophyllous vegetation	9	Mixed Shrubland/Grassland
3.2.4	Transitional woodland-shrub	9	Mixed Shrubland/Grassland
3.3.1	Beaches, dunes, sands	19	Barren or Sparsely Vegetated
3.3.2	Bare rocks	19	Barren or Sparsely Vegetated
3.3.3	Sparsely vegetated areas	19	Barren or Sparsely Vegetated
3.3.4	Burnt areas	19	Barren or Sparsely Vegetated
3.3.5	Glaciers and perpetual snow	24	Snow or Ice
4.1.1	Inland marshes	17	Herbaceous Wetland
4.1.2	Peat bogs	17	Herbaceous Wetland
4.2.1	Salt marshes	17	Herbaceous Wetland
4.2.2	Salines	17	Herbaceous Wetland
4.2.3	Intertidal flats	17	Herbaceous Wetland
5.1.1	Water courses	16	Water Bodies
5.1.2	Water bodies	28	Water Bodies
5.2.1	Coastal lagoons	28	Water Bodies
5.2.2	Estuaries	16	Water Bodies
5.2.3	Sea and ocean	16	Water Bodies

Table AT2: Scheme used to map the Urban classes from CLC into the USGS categories.

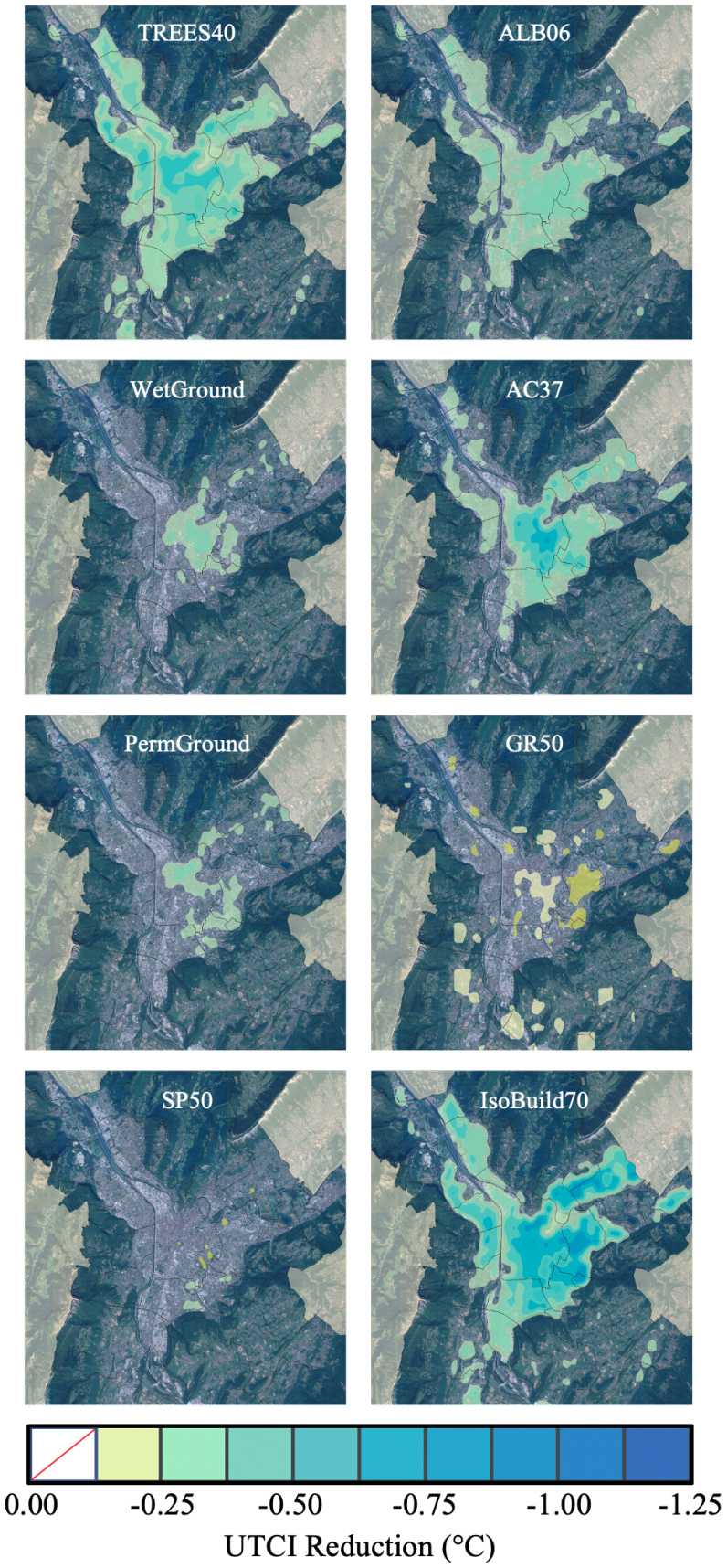

Figure AF1: Spatial distribution of median daytime UTCI reductions for each adaptation scenario during the 2023 Grenoble heatwave.

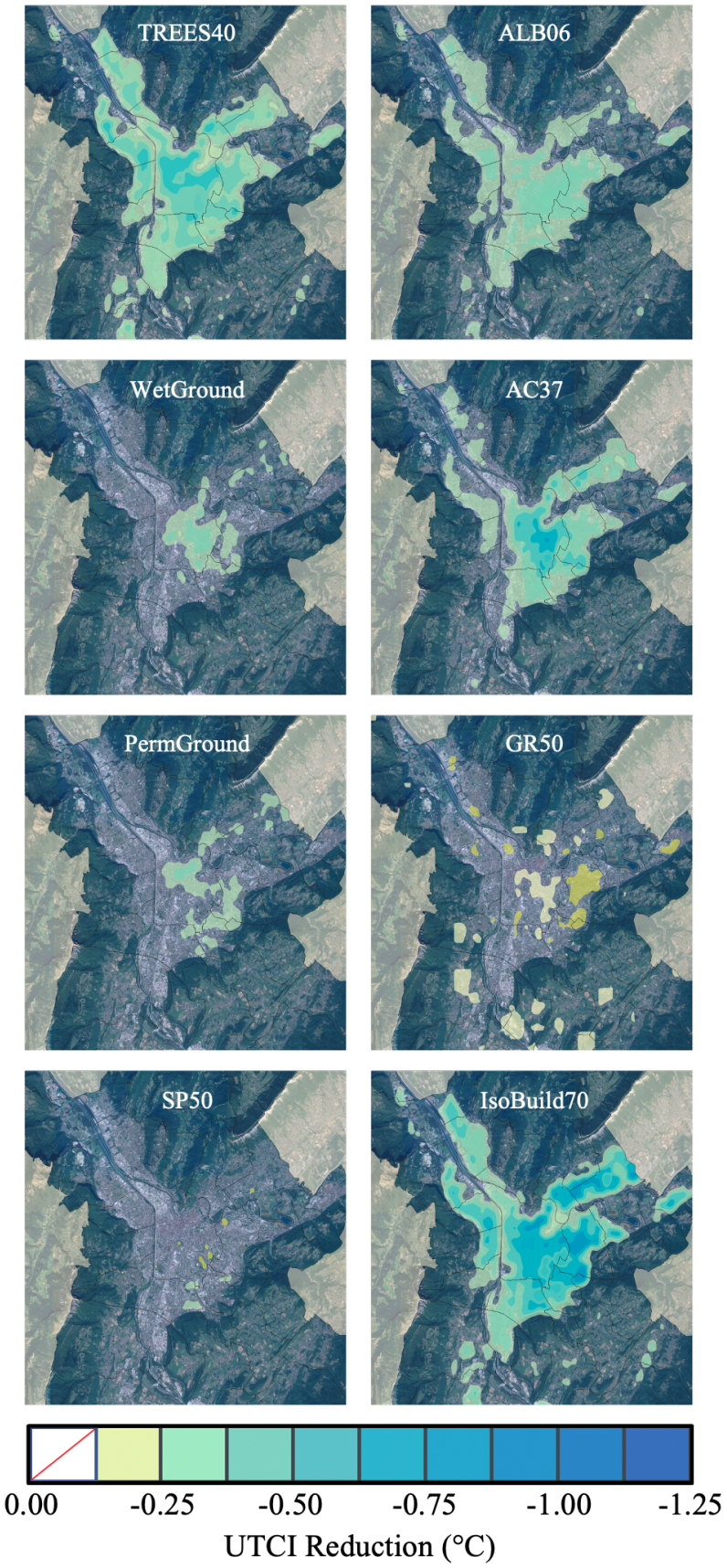

Figure AF2: Spatial distribution of median UTCI reductions for each adaptation scenario during the 2023 Grenoble heatwave.

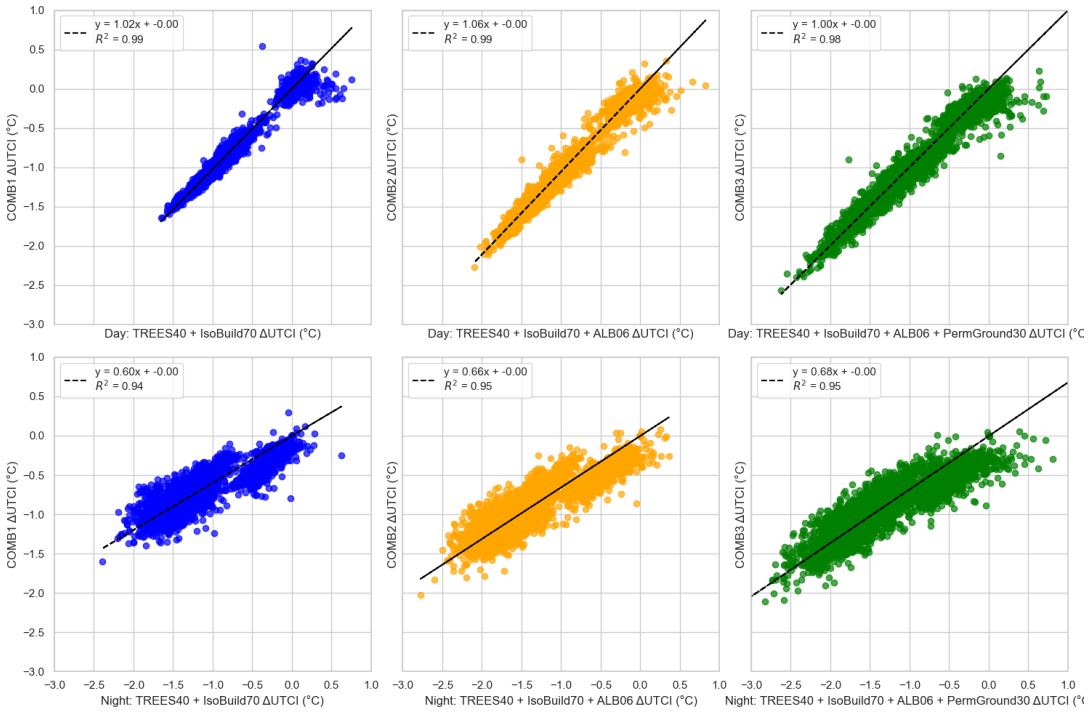

Figure AF3: Scatter plots comparing temperature reductions of combined scenarios (COMB1, COMB2, and COMB3) with their respective constituent scenarios. The top row represents daytime comparisons, while the bottom row represents nighttime comparisons.

Table AT3: Energy consumption and savings for various adaptation scenarios during the 2023 Grenoble heatwave (adjusted values).

Scenario	**Energy (GWh)**	**Relative Cons. (%)**	**Peak Cons. (GW)**	**Relative Peak Cons. (%)**
Control	80.60	100.00	0.45	100.00
AC37	28.86	35.89	0.16	36.53
ALB06	63.86	76.95	0.38	85.51
GR50	74.27	90.87	0.41	90.34
IsoBuild70	58.44	68.64	0.31	69.72
PermGround30	76.84	95.28	0.44	97.49
SP50	73.59	90.68	0.41	91.65
TREES40	60.19	73.66	0.37	81.64
WetGround	79.88	98.90	0.44	98.43
COMB1	44.48	50.42	0.25	56.75
COMB2	35.98	39.97	0.22	49.97
COMB3	34.00	37.75	0.22	48.49

References

ADEME. (2020). *Rafraîchir les villes: Solutions pour s'adapter au changement climatique*. Agence de la Transition Écologique. https://librairie.ademe.fr/changement-climatique/4649-rafraichir-les-villes.html
Accessed: February 2025.

Alexandri, E., & Jones, P. (2008). Temperature decreases in an urban canyon due to green walls and green roofs in diverse climates. *Building and Environment*, *43*(4), 480–493. https://doi.org/10.1016/j.buildenv.2006.10.055

Balany, F., Ng, A. W., Muttil, N., Muthukumaran, S., & Wong, M. S. (2020). Green Infrastructure as an Urban Heat Island Mitigation Strategy—A Review. *Water*, *12*(12), 3577. https://doi.org/10.3390/w12123577

Ballester, J., Quijal-Zamorano, M., Méndez Turrubiates, R. F., Pegenaute, F., Herrmann, F. R., Robine, J. M., Basagaña, X., Tonne, C., Antó, J. M., & Achebak, H. (2023). Heat-related mortality in Europe during the summer of 2022. *Nature Medicine*, *29*(7), 1857–1866. https://doi.org/10.1038/s41591-023-02419-z

Blessing Aibhamen Edeigba, Ugochukwu Kanayo Ashinze, Aniekan Akpan Umoh, Preye Winston Biu, & Andrew Ifesinachi Daraojimba. (2024). Urban green spaces and their impact on environmental health: A Global Review. *World Journal of Advanced Research and Reviews*, *21*(2), 917–927. https://doi.org/10.30574/wjarr.2024.21.2.0518

Bougeault, P., & Lacarrere, P. (1989). Parameterization of Orography-Induced Turbulence in a Mesobeta–Scale Model. *Monthly Weather Review*, *117*(8), 1872–1890. https://doi.org/10.1175/1520-0493(1989)117<1872:POOITI>2.0.CO;2

Bröde, P., Fiala, D., Błażejczyk, K., Holmér, I., Jendritzky, G., Kampmann, B., Tinz, B., & Havenith, G. (2012). Deriving the operational procedure for the Universal Thermal Climate Index (UTCI). *International Journal of Biometeorology*, *56*(3), 481–494. https://doi.org/10.1007/s00484-011-0454-1

Burger, M., Gubler, M., & Brönnimann, S. (2022). Modeling the intra-urban nocturnal summertime air temperature fields at a daily basis in a city with complex topography (J. Yang, Ed.). *PLOS Climate*, *1*(12), e0000089. https://doi.org/10.1371/journal.pclm.0000089

ClimaMeter. (2023). Late summer French heatwave - August 2023 [Published: ClimaMeter Research Reports]. https://www.climameter.org/20230820-23-late-summer-french-heatwave
Accessed: 2025-02-03.

Copernicus Climate Change Service. (2023). August 2023, second warmest month closes the warmest summer. https://climate.copernicus.eu/august-2023-second-warmest-month-closes-warmest-summer

Daniel, M., Lemonsu, A., Déqué, M., Somot, S., Alias, A., & Masson, V. (2019). Benefits of explicit urban parameterization in regional climate modeling to study climate and city interactions. *Climate Dynamics*, *52*(5-6), 2745–2764. https://doi.org/10.1007/s00382-018-4289-x

Demuzere, M., Bechtel, B., Middel, A., & Mills, G. (2019). Mapping Europe into local climate zones (M. Mourshed, Ed.). *PLOS ONE*, *14*(4), e0214474. https://doi.org/10.1371/journal.pone.0214474

Demuzere, M., Kittner, J., & Bechtel, B. (2021). LCZ Generator: A Web Application to Create Local Climate Zone Maps. *Frontiers in Environmental Science*, *9*, 637455. https://doi.org/10.3389/fenvs.2021.637455

Dominguez, A., Kleissl, J., & Luvall, J. C. (2011). Effects of solar photovoltaic panels on roof heat transfer. *Solar Energy*, *85*(9), 2244–2255. https://doi.org/10.1016/j.solener.2011.06.010

Esch, T., Brzoska, E., Dech, S., Leutner, B., Palacios-Lopez, D., Metz-Marconcini, A., Marconcini, M., Roth, A., & Zeidler, J. (2022). World Settlement Footprint 3D - A first three-dimensional survey of the global building stock. *Remote Sensing of Environment*, *270*, 112877. https://doi.org/10.1016/j.rse.2021.112877

European Environment Agency. (2019). CORINE Land Cover 2018 (vector), Europe, 6-yearly - version 2020_20u1, May 2020. https://doi.org/10.2909/71C95A07-E296-44FC-B22B-415F42ACFDF0

Gabeiras, J. (2024). Wrfup: A Python package for urban parameter ingestion in WRF. https://github.com/jacobogabeiraspenas/wrfup
Accessed: 2024-05-15.

Gabeiras, J. (2025). UrbanData01: High-resolution urban datasets for WRFUP package. https://github.com/jacobogabeiraspenas/UrbanData01
Accessed: 2025-02-06.

Gallo, E., Quijal-Zamorano, M., Méndez Turrubiates, R. F., Tonne, C., Basagaña, X., Achebak, H., & Ballester, J. (2024). Heat-related mortality in Europe during 2023 and the role of adaptation in protecting health. *Nature Medicine*, *30*(11), 3101–3105. https://doi.org/10.1038/s41591-024-03186-1

Han, D., Zhang, T., Qin, Y., Tan, Y., & Liu, J. (2023). A comparative review on the mitigation strategies of urban heat island (UHI): A pathway for sustainable urban development. *Climate and Development*, *15*(5), 379–403. https://doi.org/10.1080/17565529.2022.2092051

Haroun, B., Bahreini, G., Zaman, M., Jang, E., Okoye, F., Elbeshbishy, E., Santoro, D., Walton, J., Al-Omari, A., Muller, C., Bell, K., & Nakhla, G. (2022). Vacuum-enhanced anaerobic fermentation: Achieving process intensification, thickening and improved hydrolysis and VFA yields in a single treatment step. *Water Research*, *220*, 118719. https://doi.org/10.1016/j.watres.2022.118719

Hasan, F., Marsia, S., Patel, K., Agrawal, P., & Razzak, J. A. (2021). Effective Community-Based Interventions for the Prevention and Management of Heat-Related Illnesses: A Scoping Review. *International Journal of Environmental Research and Public Health*, *18*(16), 8362. https://doi.org/10.3390/ijerph18168362

Hatvani-Kovacs, G., & Boland, J. (2015). Retrofitting Precincts for Heatwave Resilience: Challenges and Barriers in Australian Context. *Challenges*, *6*(1), 3–25. https://doi.org/10.3390/challe6010003

Ibsen, P. C., Jenerette, G. D., Dell, T., Bagstad, K. J., & Diffendorfer, J. E. (2022). Urban landcover differentially drives day and nighttime air temperature across a semi-arid city. *Science of The Total Environment*, *829*, 154589. https://doi.org/10.1016/j.scitotenv.2022.154589

Knight, T., Price, S., Bowler, D., Hookway, A., King, S., Konno, K., & Richter, R. L. (2021). How effective is 'greening' of urban areas in reducing human exposure to ground-level ozone concentrations, UV exposure and the 'urban heat island effect'? An updated systematic review. *Environmental Evidence*, *10*(1), 12. https://doi.org/10.1186/s13750-021-00226-y

Kwon, C., & Lee, K. (2017). Outdoor Thermal Comfort in a Transitional Space of Canopy in Schools in the UK. *Sustainability*, *9*(10), 1753. https://doi.org/10.3390/su9101753

Larsen, L. (2015). Urban climate and adaptation strategies. *Frontiers in Ecology and the Environment*, *13*(9), 486–492. https://doi.org/10.1890/150103

Le Monde. (2023). French heatwave sets new late-summer record. https://www.lemonde.fr/en/environment/article/2023/08/23/french-heatwave-sets-new-late-summer-record_6104929_114.html

Le Monde. (2024). France recorded over 5,000 deaths due to summer 2023 heat. https://www.lemonde.fr/en/france/article/2024/02/08/france-recorded-over-5-000-deaths-due-to-summer-2023-heat_6505713_7.html

Lee, S., Cho, Y.-I., Lee, M.-J., & Lim, Y.-S. (2023). The Evaluation of the Temperature Reduction Effects of Cool Roofs and Cool Pavements as Urban Heatwave Mitigation Strategies. *Applied Sciences*, *13*(20), 11451. https://doi.org/10.3390/app132011451

Li, D., Bou-Zeid, E., & Oppenheimer, M. (2014). The effectiveness of cool and green roofs as urban heat island mitigation strategies. *Environmental Research Letters*, *9*(5), 055002. https://doi.org/10.1088/1748-9326/9/5/055002

Li, H., Zhao, Y., Wang, C., Ürge-Vorsatz, D., Carmeliet, J., & Bardhan, R. (2024). Cooling efficacy of trees across cities is determined by background climate, urban morphology, and tree trait. *Communications Earth & Environment*, *5*(1), 754. https://doi.org/10.1038/s43247-024-01908-4

Liao, W., Liu, X., Li, D., Luo, M., Wang, D., Wang, S., Baldwin, J., Lin, L., Li, X., Feng, K., Hubacek, K., & Yang, X. (2018). Stronger Contributions of Urbanization to Heat Wave Trends in Wet Climates. *Geophysical Research Letters*, *45*(20). https://doi.org/10.1029/2018GL079679

Lowe, D., Ebi, K. L., & Forsberg, B. (2011). Heatwave Early Warning Systems and Adaptation Advice to Reduce Human Health Consequences of Heatwaves. *International Journal of Environmental Research and Public Health*, *8*(12), 4623–4648. https://doi.org/10.3390/ijerph8124623

Marcotullio, P. J., Keßler, C., & Fekete, B. M. (2022). Global urban exposure projections to extreme heatwaves. *Frontiers in Built Environment*, *8*, 947496. https://doi.org/10.3389/fbuil.2022.947496

Martilli, A., Clappier, A., & Rotach, M. W. (2002). An Urban Surface Exchange Parameterisation for Mesoscale Models. *Boundary-Layer Meteorology*, *104*(2), 261–304. https://doi.org/10.1023/A:1016099921195

Martilli, A., Nazarian, N., Krayenhoff, E. S., Lachapelle, J., Lu, J., Rivas, E., Rodriguez-Sanchez, A., Sanchez, B., & Santiago, J. L. (2024). WRF-Comfort: Simulating microscale variability in outdoor heat stress at the city scale with a mesoscale model. *Geoscientific Model Development*, *17*(12), 5023–5039. https://doi.org/10.5194/gmd-17-5023-2024

Mazdiyasni, O., Sadegh, M., Chiang, F., & AghaKouchak, A. (2019). Heat wave Intensity Duration Frequency Curve: A Multivariate Approach for Hazard and Attribution Analysis. *Scientific Reports*, *9*(1), 14117. https://doi.org/10.1038/s41598-019-50643-w

Météo-France. (2023). Fortes chaleurs d'août 2023. https://meteofrance.com/actualites-et-dossiers/actualites/fortes-chaleurs-aout-2023
Accessed: 2024-02-02.

Métropole, G. A. (2018). *Energy-Climate Roadmap 2050* (tech. rep.). Grenoble Alpes Métropole. https://www.citiesoftomorrow.eu/sites/default/files/documents/Grenoble_Energy-Climate-Roasmap-2050_2018_en.pdf

Métropole, G. A. (2023). *Sustainable Development Report* (tech. rep.). Grenoble Alpes Métropole. https://www.grenoblealpesmetropole.fr/cms_viewFile.php?idtf=3026&path=Rapport-dev-durable-2023.pdf

Mlawer, E. J., Taubman, S. J., Brown, P. D., Iacono, M. J., & Clough, S. A. (1997). Radiative transfer for inhomogeneous atmospheres: RRTM, a validated correlated-k model for the longwave. *Journal of Geophysical Research: Atmospheres*, *102*(D14), 16663–16682. https://doi.org/10.1029/97JD00237

Nairn, J., & Fawcett, R. (2014). The Excess Heat Factor: A Metric for Heatwave Intensity and Its Use in Classifying Heatwave Severity. *International Journal of Environmental Research and Public Health*, *12*(1), 227–253. https://doi.org/10.3390/ijerph120100227

Pappaccogli, G., Giovannini, L., Zardi, D., & Martilli, A. (2021). Assessing the Ability of WRF-BEP + BEM in Reproducing the Wintertime Building Energy Consumption of an Italian

Alpine City. *Journal of Geophysical Research: Atmospheres*, *126*(8), e2020JD033652. https://doi.org/10.1029/2020JD033652

Patel, P., & Roth, M. (2022, August). A High-Resolution Dataset of Global Urban Fraction for Mesoscale Urban Modelling. https://doi.org/10.5281/ZENODO.6994974

Perkins, S. E., Alexander, L. V., & Nairn, J. R. (2012). Increasing frequency, intensity and duration of observed global heatwaves and warm spells. *Geophysical Research Letters*, *39*(20), 2012GL053361. https://doi.org/10.1029/2012GL053361

Perkins-Kirkpatrick, S. E., & Lewis, S. C. (2020). Increasing trends in regional heatwaves. *Nature Communications*, *11*(1), 3357. https://doi.org/10.1038/s41467-020-16970-7

Razzak, J. A., Agrawal, P., Chand, Z., Quraishy, S., Ghaffar, A., & Hyder, A. A. (2022). Impact of community education on heat-related health outcomes and heat literacy among low-income communities in Karachi, Pakistan: A randomised controlled trial. *BMJ Global Health*, *7*(1), e006845. https://doi.org/10.1136/bmjgh-2021-006845

Renard, F., Alonso, L., Fitts, Y., Hadjiosif, A., & Comby, J. (2019). Evaluation of the Effect of Urban Redevelopment on Surface Urban Heat Islands. *Remote Sensing*, *11*(3), 299. https://doi.org/10.3390/rs11030299

Réseau d'Observation Météorologique du Massif Alpin (ROMMA). (2023). Grenoble Climate Data – August 2023. https://www.romma.fr/station_clim_mois.php?id=4&month=8&year=2023
Accessed: 2024-02-02.

Salamanca, F., Georgescu, M., Mahalov, A., Moustaoui, M., & Martilli, A. (2016). Citywide Impacts of Cool Roof and Rooftop Solar Photovoltaic Deployment on Near-Surface Air Temperature and Cooling Energy Demand. *Boundary-Layer Meteorology*, *161*(1), 203–221. https://doi.org/10.1007/s10546-016-0160-y

Salamanca, F., Krpo, A., Martilli, A., & Clappier, A. (2010). A new building energy model coupled with an urban canopy parameterization for urban climate simulations—part I. formulation, verification, and sensitivity analysis of the model. *Theoretical and Applied Climatology*, *99*(3-4), 331–344. https://doi.org/10.1007/s00704-009-0142-9

Schmidt, K., & Walz, A. (2021). Ecosystem-based adaptation to climate change through residential urban green structures: Co-benefits to thermal comfort, biodiversity, carbon storage and social interaction. *One Ecosystem*, *6*, e65706. https://doi.org/10.3897/oneeco.6.e65706

Schmidt, V. (2024). Urban morphology as a key parameter for mitigating urban heat? – A literature review. *IOP Conference Series: Earth and Environmental Science*, *1363*(1), 012074. https://doi.org/10.1088/1755-1315/1363/1/012074

Schneider, M. (2022). Observations et Modélisation du Climat en France: Évolution et Perspectives [Published: Presentation at AIC Conference]. http://www.meteo.fr/cic/meetings/2022/aic/presentations/obs_model_schneider.pdf
Accessed: 2024-02-02.

United Nations Department of Economic and Social Affairs. (2019, August). *World Urbanization Prospects: The 2018 Revision*. UN. https://doi.org/10.18356/b9e995fe-en

Van Oorschot, J., Slootweg, M., Remme, R. P., Sprecher, B., & Van Der Voet, E. (2024). Optimizing green and gray infrastructure planning for sustainable urban development. *npj Urban Sustainability*, *4*(1), 41. https://doi.org/10.1038/s42949-024-00178-5

Wang, X. Y., Barnett, A. G., Yu, W., FitzGerald, G., Tippett, V., Aitken, P., Neville, G., McRae, D., Verrall, K., & Tong, S. (2012). The impact of heatwaves on mortality and emergency hospital admissions from non-external causes in Brisbane, Australia. *Occupational and Environmental Medicine*, *69*(3), 163–169. https://doi.org/10.1136/oem.2010.062141

Wang, Y., Berardi, U., & Akbari, H. (2016). Comparing the effects of urban heat island mitigation strategies for Toronto, Canada. *Energy and Buildings*, *114*, 2–19. https://doi.org/10.1016/j.enbuild.2015.06.046

Yuan, T. (2024). The Role of Green Infrastructure in Mitigating the Urban Heat Island Effect. *Open Journal of Applied Sciences*, *14*(11), 3155–3164. https://doi.org/10.4236/ojapps.2024.1411207

Zhu, L., Yang, J., Ouyang, X., Xu, Y., Wong, M. S., & Menenti, M. (2024). Street trees: The contribution of latent heat flux to cooling dense urban areas. *Urban Climate*, *58*, 102147. https://doi.org/10.1016/j.uclim.2024.102147

Zonato, A., Martilli, A., Gutierrez, E., Chen, F., He, C., Barlage, M., Zardi, D., & Giovannini, L. (2021). Exploring the Effects of Rooftop Mitigation Strategies on Urban Temperatures and Energy Consumption. *Journal of Geophysical Research: Atmospheres*, *126*(21), e2021JD035002. https://doi.org/10.1029/2021JD035002